To the Graduate Council:

I am submitting herewith a thesis written by Aquilino B. Orichi-Batajolo entitled "Performance of a Frequency Hop Spread Spectrum Multiple Access Radio Network in a Factory Environment." I have examined the final copy of this for form and content and recommend that it be accepted in partial fulfillment of the requirements for the degree of Master of Science, with a major in Electrical Engineering.

Daniel B. Koch

Daniel B. Koch, Major Professor

We have read this thesis
and recommend its acceptance:

J. W. Wallace

Herbert S. Ruff Jr.

Accepted for the Council:

Associate Vice Chancellor
and Dean of Graduate School

STATEMENT OF PERMISSION TO USE

In presenting this thesis in partial fulfillment of the requirements for a Master's degree at The University of Tennessee, Knoxville, I agree that the Library shall make it available to borrowers under rules of the Library. Brief quotations from this thesis are allowable without special permission, provided that accurate acknowledgment of the source is made.

Permission for extensive quotation from or reproduction of this thesis may be granted by my major professor, or in his absence, by the Head of Interlibrary Services when, in the opinion of either, the proposed use of the material is for scholarly purposes. Any copying or use of the material in this thesis for financial gain shall not be allowed without my written permission.

Signature Aquilino B. Oriclu-Batajo

Date 7/15/'94

Performance of a Frequency Hop Spread Spectrum Multiple Access Radio Network in a Factory Environment

A Thesis

Presented for the

Master of Science

Degree

The University of Tennessee, Knoxville

Aquilino B. Orichi-Batajolo

August 1994

To My Parents

Luis Orichi

and

Rufina Batajolo

Acknowledgment

I would like to express my deepest gratitude and sincere appreciation to my major professor, Dr. Daniel B. Koch, for his invaluable support and patience throughout this study. I would also like to thank Dr. Herbert P. Neff and Dr. J. W. Waller for their advice and comments as members of my graduate committee. In addition, I wish to thank to IEEE for permitting me to reprint three figures from IEEE publications.

Special thanks should go to my parents, Luis Orichi and Rufina Batajolo, my uncles, Silvestre Orichi and Claudio Batajolo, and my brothers for their love and encouragement.

Finally, I thank Debbie for her understanding and Eric Wrushen, Alireza Hajialigol, and the other members of the CISP group for their friendship and encouragement.

Abstract

Wireless indoor networks provide terminal portability to any node in the network and promise to reduce significantly the expense and troubles associated with wired networks. Since wireless systems operate on band-limited channels and have to adjust to constant fluctuations of the indoor environment (i.e. multipath and intermittent fading), any viable wireless technology should be able to accommodate those constraints. A very attractive wireless technology for indoor networks is spread spectrum because of its ability to mitigate multipath fading and incorporate multiple access for bandwidth efficient sharing.

A simulated model for a noncoherent FH/BFSK spread spectrum multiple access indoor radio network in a factory environment will be developed in this thesis. The system will be evaluated based on the bit error rate (BER) performance for various number of users, number of hopping frequencies, and different chip rates for a given signal to noise plus interference density ratio. Normally, extensive site measurements have to be taken for accurate behavior of a wireless system, but for simulation purposes, there are widely accepted lower and upper BER approximations for any given interference or noise constraint. The results of this work will be compared to the upper and lower bounds mentioned earlier. This work represents the culmination of a nine month study.

Table of Contents

CHAPTER			PAGE
1.	INTRODUCTION		1
2.	SPREAD SPECTRUM TECHNIQUES		5
	2.1	Spread Spectrum Overview	5
	2.2	Pseudonoise Sequences	8
	2.3	Gold Codes	11
	2.4	Direct Sequence Spread Spectrum	14
	2.5	Frequency Hopping Spread Spectrum	19
	2.6	Other Spread Spectrum Techniques	20
	2.7	Spread Spectrum and CDMA	21
3.	INDOOR RADIO PROPAGATION CHARACTERISTICS		23
	3.1	Introduction	23
	3.2	Multipath Propagation Model	24
	3.3	Indoor Channel Propagation Measurements	28
4.	FH/BFSK/CDMA SIMULATION PROGRAM FOR THE FACTORY ENVIRONMENT		36
	4.1	System Design Considerations	37
	4.2	System Simulation	40
	4.3	Simulation Program	41
5.	FH/BFSK/CDMA PERFORMANCE		63
	5.1	Performance Evaluation	63
	5.2	Experimental Results	66
6.	CONCLUSION		72
LIST OF REFERENCES			74
VITA			77

List of Figures

FIGURE		PAGE
2.1	Conceptual spread spectrum system (a) transmitter (b) receiver	7
2.2	General binary shift register circuit with n stages	9
2.3	Autocorrelation of : (a) random binary sequence (b) PN sequence	10
2.4	Two shift register Gold code generator configuration	11
2.5	5-stage Gold code generator	12
2.6	NRZ pulse waveform of (a) message signal (b) PN sequence	15
2.7	DS/SS BFSK system (a) transmitter (b) receiver	16
2.8	Spectra of desired signal and interference (a) receiver input (b) despreading demodulator output	19
2.9	Frequency synthesizer output for four different 3-bit words	20
3.1	Multi-ray propagation model	23
3.2	Rician pdf	27
3.3	Rayleigh pdf	27
3.4	Multipath delay profile from one location on a manufacturing floor	32
3.5	Variation of RMS delay spread (ns)	33
3.6	Variation of multipath power (dB)	34
4.1	FH/BFSK/CDMA system (a) transmitter (b) channel (c) receiver	39
4.2	FH/BFSK/CDMA system	42
4.3	Transmitter VI	46
4.4	"BFSK" Encoder Sub-VI	48
4.5	"Gold Code Generator" Sub-VI	49

4.6	{7,3} and {7,1} m-length Gold code generator	50
4.7	"User's Bank Code" sub-VI	52
4.8	"Frequency Synthesizer" Sub-VI	53
4.9	"Spreader" Sub-VI	55
4.10	"Channel" Sub-VI	57
4.11	"AWGN" Sub-VI	58
4.12	"Receiver" Sub-VI	60
4.13	Schematic representation of a quadrature receiver	62
5.1	Theoretical and simulated BER for L=10, K=1, p=20, 1 hop/bit	66
5.2	Theoretical and simulated BER for L=10, K=6, p=20, 1 hop/bit	67
5.3	Theoretical and simulated BER for L=10, K=6, p=60, 1 hop/bit	68
5.4	Theoretical and simulated BER for L=10, K=6, p=60, 5 hops/bit	66
5.1	Theoretical and simulated BER for L=10, K=6, p=60, 3 bits/hop	66

Chapter 1

Introduction

Wireless networks have traditionally been the domain of wide area voice networks (i.e., microwave and satellite). However, in recent years, they are beginning to influence local area networks (LANs) and private branch exchanges (PBXs) in indoor networks. Generally indoor networks use either existing telephone networks or require the addition of cable, wires, and fiber-optic LANs to interconnect various equipment for optimum transfer of information and efficient sharing of common resources such as printers and mass storage devices. Since wires and cable are the backbone of current indoor networks, installation, relocation, and expansion of these systems are difficult and expensive. Some studies suggest that the installation cost for copper cabling can reach up to $1,000 per node; coax and fiber-optic costs run considerably higher [1]. In addition, the frequent additions and changes of terminals and other equipment in today's workplace, in order to increase productivity and competitiveness, further add to the aforementioned costs. Structured distribution systems (SDS) have helped lower the cost and troubles associated with wiring [2], but there will always be environments where wiring is difficult, such as historic buildings and offices without drop ceilings to name a few. Given the expense and shortcomings of physical cabling, the concept of wireless indoor networks becomes an attractive alternative.

Wireless indoor networks can alleviate the cost and difficulties of wiring and rewiring within buildings as well as provide terminal portability to any node in the network. To claim the attribute of portability, wireless indoor networks should be easy to install and change, so that terminals and other equipment may

be moved around freely at the convenience of the user. It is imperative then that wireless networks be compatible with existing networks in terms of physical and logical interfaces in a way that is virtually transparent to the operating system and application software [2]. Experts agree that the success of these networks in penetrating the indoor arena will depend on their flexibility, cost effectiveness, and competitive performance with wired networks.

Cost and performance go hand in hand for any emerging technology. Potential customers can appreciate technology, but what they ultimately shop for is acceptable performance for their needs at a reasonable price. Therefore, wireless networks should be cost compatible with installation and relocation costs of wired systems in the long run. Indeed, in working environments where there is an ever increasing number of terminals and frequent relocation of office workers (e.g., accounting and marketing departments), wireless networks can be a cost effective solution [3]. Beyond costs, performance is another big factor. Wireless networks are expected to support the 10 Mb/s speed adequate for today's wired LANs and higher speed envisioned for the future, offer low delay, good reliability and security against unauthorized users.

Two basic technologies are currently used to implement wireless networks. These are: infrared (IR) and radio frequency (RF). IR systems operate in that part of the electromagnetic spectrum just below visible light--about 10^5 GHz -- and RF systems are located below 300 GHz [3]. Since electromagnetic wave depth of penetration is inversely proportional to frequency, IR signals cannot pass through most objects but radio signals can. Therefore, the choice between IR and RF to implement a wireless in-building network depends on the coverage area, building architecture, construction materials, and channel noise characteristics. For example, RF may be the technology of choice for a multi-story building where the covered area is defined by a number of floors and the signal

must pass through the walls. IR may be more attractive for open working environments with considerable noise at radio frequencies.

The indoor environment is very hostile to radio propagation due to multipath fading caused by multiple reflected copies of the same signal arriving from different paths, and intermittent signal blockage which results from moving obstacles such as people or doors. The effect of these disturbances is performance degradation. Thus, any wireless network technology should be able to adjust to the constant fluctuation of the indoor environment. This requirement makes wireless networks very complicated to design. A wireless network designer has to pay close attention to measurements of channel parameters such as RMS delay spread and multipath profiles to assess the feasibility of a given design. In addition, the limited bandwidth available for radio systems calls for a bandwidth efficient modulation technique for greater utilization of scarce communication resources and compliance with Federal Communications Commission (FCC) regulations and industrial technology standards.

The work presented here evaluates the performance of a Frequency Hop (FH) Spread Spectrum Multiple Access communication system in office and factory environments. Spread spectrum signaling techniques are particularly suitable for indoor applications because of their ability to mitigate the effect of multipath fading, operate in parallel with other existing RF systems, and to provide resistance to intentional interference [3,4]. The general problem of spread spectrum systems is that they employ a transmission bandwidth much larger than the minimum required to transmit information. Thus, to overcome the apparent bandwidth inefficient utilization, a Code Division Multiple Access (CDMA) technique is used to allow various terminals to share simultaneously the same bandwidth. Each terminal is assigned a different orthogonal spreading code to reduce the amount of mutual interference among terminals sharing the

same bandwidth. As more terminals are added, the mutual interference increases; so does the bit error rate (BER). Since BER depends on the bit energy to noise plus interference density ratio [5], a good measure of performance is the number of terminals that can be allocated for a given bandwidth without going below a threshold BER for a given bit energy to noise plus interference ratio. Thus, a clear picture of system behavior may be based on BER performance for various chip rates, data rates, and number of hopping frequencies -- for frequency hop systems -- for a given signal to noise plus interference ratio.

A brief outline of the organization of this thesis is as follows. Chapter 2 is an overview of spread spectrum multiple access techniques and their applications. The characteristics of indoor radio channels and effects of the disturbances observed in these channels is presented in Chapter 3. The system model and software simulation is presented in Chapter 4. The system performance evaluation can be found in Chapter 5. Finally, Chapter 6 presents the conclusions of this work and suggestions for future research.

Chapter 2

Spread Spectrum Techniques

2.1 Spread Spectrum Overview

Spread Spectrum (SS) is a technique that uniformly distributes the information bandwidth of a voice or data signal over a frequency range that is much larger than that required for transmission. Nyquist's bandwidth constraint criterion states that the theoretical minimum required bandwidth to send an information signal without intersymbol interference (ISI) is twice that required for the information itself [5]. ISI occurs when two adjacent signals overlap at the receiver causing performance degradation. Thus, based on Nyquist's bandwidth criterion, a voice signal (300 to 3300 Hz) may be sent, with some degradation, by conventional amplitude modulation in a bandwidth just twice that of the information itself; that is about 6600 Hz. However, the same voice signal transmitted with spread spectrum in the 900 MHz frequency range as established by FCC Part 15.274 for unlicensed used of SS requires 26 MHz of bandwidth [6].

There are several specific modulation techniques that can fall under the umbrella of SS. These include FM systems with deviation ratios greater than one and wideband AM systems, but the name SS is generally reserved for the family of techniques that generate wideband signals under the control of a pseudonoise (PN) sequence or pseudonoise code. PN sequences are actually periodic and deterministic but have random-like characteristics. As a result, SS signals appear as random-like signals with unique characteristics:

- They can provide great resistance to intentional interference (i.e., jamming) because the transmitted power can be distributed in

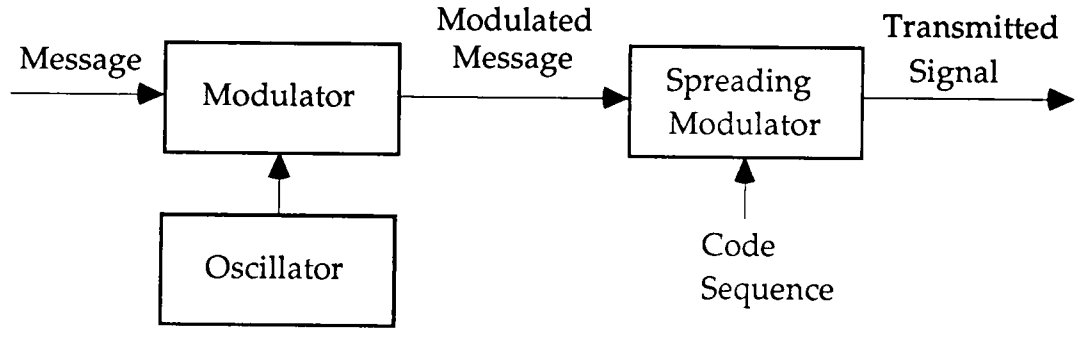
different portions of the total available frequency band for a short period of time (FH/SS). Thus, a knowledge of the transmitted distribution power in the different portions of the frequency band is required to successfully destroy an SS transmission. This is only possible with a complete knowledge of the PN sequence or by jamming the total band with excessive power--an approach which will prove to be very costly.

- They can be very difficult to detect or intercept by an adversary receiver because the signals appear noise-like. A simple narrow band receiver rejects spread spectrum signals as another type of noise; a radiometer which is a receiver that can detect the smallest concentration of power, is able to detect their presence. However, the actual detection of spread spectrum poses more difficulty since it is necessary to produce an exact replica of the PN sequence at the receiver in order to successfully extract information.
- Other users may operate in the same frequency band simultaneously by using distinct spreading codes with minimal interference between all of the users, thus allowing for multiple access. This process is called Code Division Multiple Access (CDMA). More will be said about this subject in Section 2.5.

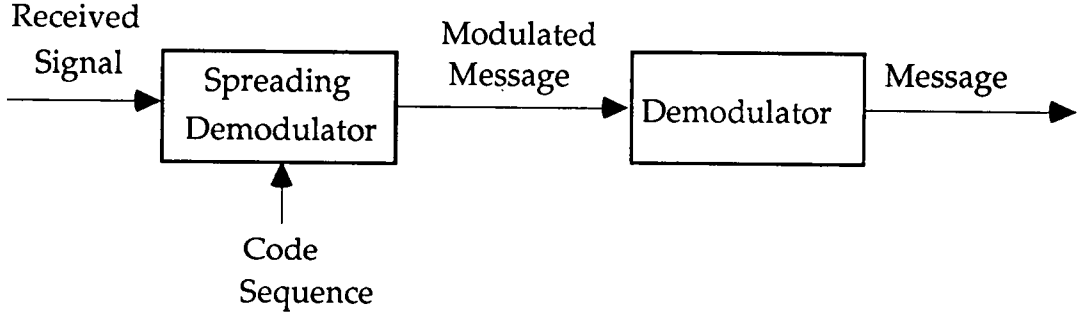
In view of the characteristics above, SS signaling provides signal protection, message privacy, and allows efficient sharing of communication resources with other users.

The process of SS modulation can be best illustrated with the aid of Figure 2.1. At the transmitter (Figure 2.1a), the message signal is first modulated onto a carrier using a conventional modulator (e.g., ASK, PSK, FSK, etc.). Then the modulated message is multiplied by a code sequence to produce a wide band

signal, in a process known as *spreading* . The receiver (Figure 2.1b) correlates the received signal with a synchronized code sequence replica of the one at the transmitter to restore the bandwidth to its modulated size -- a process known as *despreading*. Finally, the demodulated signal is passed through a filter to recover the message signal.



(a)



(b)

Figure 2.1 Conceptual spread spectrum system (a) transmitter (b) receiver.

There are two fundamental SS modulation techniques: *direct sequence* (DS) and *frequency hop* (FH). Both techniques are very similar; the only difference is that in DS the code sequence directly modulates the data signal while in FH, the code sequence drives a frequency synthesizer to generate pseudorandomly distributed transmission frequencies. These, and other SS modulation techniques, will be explored in subsequent sections.

2.2 Pseudonoise Sequences

Pseudnoise sequences or pseudonoise (PN) codes are fundamental to spread spectrum modulation techniques. The type of code used, its length, and its bit rate determine various performance characteristics of SS systems that may be modified only by changing the PN code. As such they are worth discussing before delving into SS in more detail. PN sequences are binary and periodic with characteristics similar to truly random binary sequences [7]. A random binary sequence is one where the digits "1" or "0" have equally likely probability of occurrence.

PN sequences are generated using binary shift register circuits whose configuration determines the type and behavior of the sequence. A binary shift register circuit consists of a series of memory stages for storage and shifting and a feedback path provided by a number of feedback taps. The purpose of the feedback logic is usually modulo-2 addition. Figure 2.2 shows a block diagram of the general configuration of a binary shift register circuit. If the feedback logic is composed entirely of modulo-2 adders, the PN sequence generated is said to be linear; otherwise a non-linear sequence is generated. In this presentation, only linear sequences are considered. Linear PN sequences are classified as maximal or non-maximal.

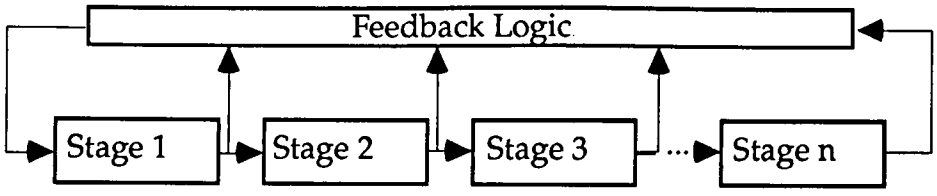
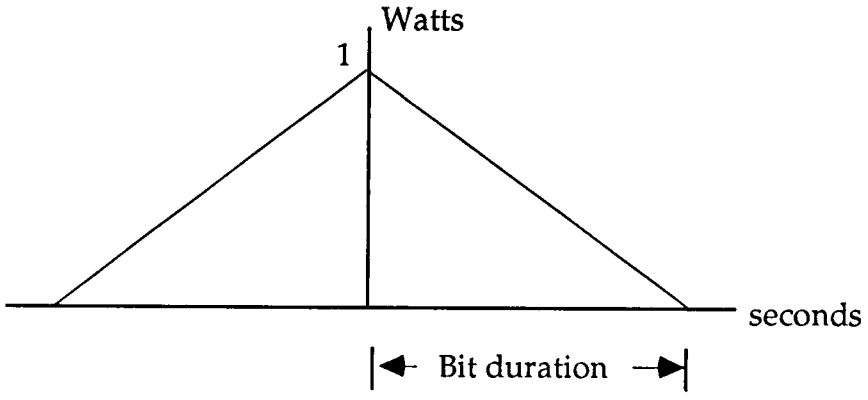


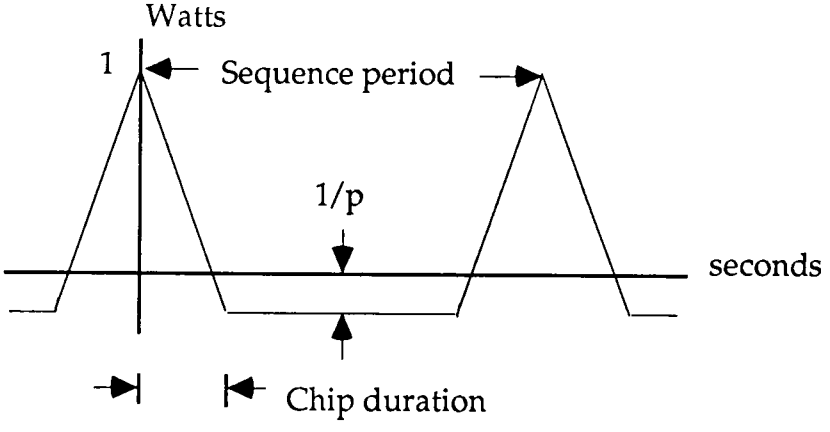
Figure 2.2 General binary shift register circuit with n stages.

Maximal linear sequences, as the name implies, are the longest that can be generated by a given binary shift register circuit. For a binary shift register circuit with n stages, the maximum length sequence length or period is $2^n - 1$ chips, (a chip is the acronym given to the bits of a PN sequence to differentiate them from data bits); that is, for a 4-stage linear binary shift register circuit the period is $2^4 - 1 = 15$ chips. The resulting autocorrelation function of these sequences closely resembles that of a random binary signal. A graphical representation of the autocorrelation function of a binary random sequence and a maximal length sequence of period p chips is shown in Figure 2.3. Observe that the peaks of the autocorrelation function of both sequences are at the beginning or at the end of the sequence period. This property allows SS receivers to select its matched code out of all others present because any code other than the one to which the receiver is matched will not produce these peaks.

In situations where a large number of codes are needed (e.g., multiple access), two maximal linear sequences may be combined to form a composite code with specific characteristics. For example, a pair of maximal code sequences may be combined in the Gold configuration to provide a large number of codes with well-defined crosscorrelation characteristics. Gold codes are very useful in SS multiple access, therefore a complete section is dedicated to these codes to explore their properties.



(a)



(b)

Figure 2.3 Autocorrelation of : (a) random binary sequence (b) PN sequence.

2.3 Gold Codes

Gold codes result from modulo-2 addition of two maximal length sequences. Figure 2.4 shows the configuration of a Gold code generator circuit. Gold codes are useful in SS multiple access because they provide a large number of codes with low crosscorrelation characteristics. The crosscorrelation, ξ, of two codes is defined as the number of agreements, A, minus the number of disagreements, D, divided by the code's period, N. This may be expressed mathematically as follows:

$$\xi = \frac{A - D}{N} \tag{2.1}$$

where

$$N = 2^n - 1 \tag{2.2}$$

and n is the number of stages of the Gold code generator circuit. As the two maximal length sequences that generate the Gold codes assume any circular shift of bits, the crosscorrelation may yield one of the possible three values [8]:

$$\xi = \begin{cases} -\frac{1}{N} h(n) & or \\ -\frac{1}{N} & or \\ \frac{1}{N}[h(n) - 2] & \end{cases} \tag{2.3}$$

where

$$h(n) = \begin{cases} 1 + 2^{(n+1)/2} & for \quad n \quad odd \\ 1 + 2^{(n+2)/2} & for \quad n \quad even \end{cases} \tag{2.4}$$

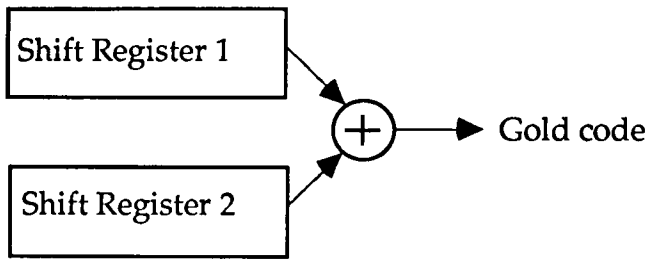


Figure 2.4 Two shift register Gold code generator configuration.

Pairs of maximum length code sequences that satisfy Equation 2.3 are referred to as preferred pairs. A preferred pair may generate up to $N + 2$ different Gold codes. As stated earlier, any circular shift of bits of the two maximal sequences generates a new Gold code. Figure 2.5 shows a 5-stage Gold code generator composed of {5, 3} and {5, 4, 3, 2} preferred pairs. The first number in the parenthesis represents the number of stages of the Gold code generator and the rest of the numbers the feedback taps that are modulo-2 added.

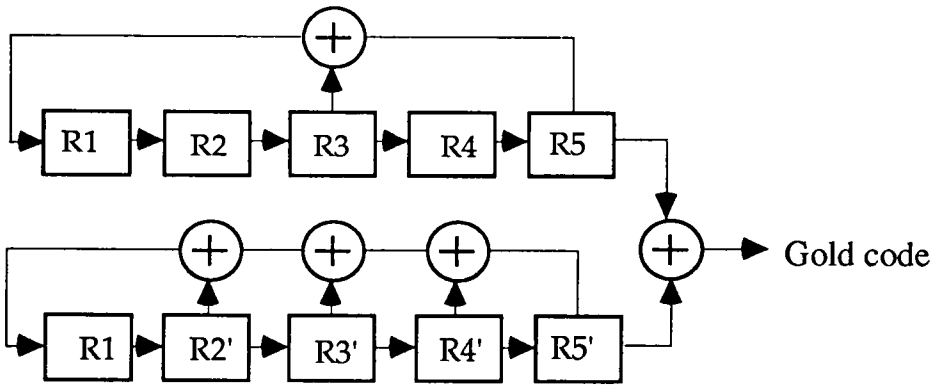


Figure 2.5 5-stage Gold code generator

Some of the Gold code properties may be observed by checking the zero-shift, one-bit-shift, and five-bit-shift combinations in the second register (represented by Rn's) from the all-ones initial conditions in both registers.

(a) zero-shift

```
  1 1 1 1 1 0 0 0 1 1 0  1 1 1 0 1 0 1 0 0 0 0 1 0 0 1 0 1 1 0 0
+ 1 1 1 1 1 0 0  1 0 0 1 1 0 0 0 0 1 0 1 1 0 1 0 1 0 0 0 1 1 1 0
  0 0 0 0 0 0 0 1 1 1 1 0 1 1  0 1 1 1 1 1 0 1 1 1 0 1 0 0 0 1 0
```

(b) one-bit-shift

```
  1 1 1 1 1 0 0 0 1 1 0 1 1 1 0 1 0 1 0 0 0 0 1 0 0 1 0 1 1 0 0
+ 1 1 1 1 0 0 1 0 0 1 1 0 0 0 0 1 0 1 1 0 1 0 1 0 0 0 1 1 1 0 1
  0 0 0 0 1 0 1 0 1 0 1 1 1 1 0 0 0 0 1 0 1 0 0 0 0 1 1 0 0 0 1
```

(c) five-bit-shift

```
  1 1 1 1 1 0 0 0 1 1 0 1 1 1 0 1 0 1 0 0 0 0 1 0 0 1 0 1 1 0 0
+ 0 0 1 0 0 1 1 0 0 0 0 1 0 1 1 0 1 0 1 0 0 0 1 1 1 0 1 1 1 1 1
  1 1 0 1 1 1 1 0 1 1 0 0 1 0 1 1 1 1 1 0 0 0 0 1 1 1 1 0 0 1 1
```

Note that thirty-one bits were considered for the modulo-2 addition (the + here represents modulo-2 addition) to produce the Gold code because the period of the codes is $2^5 - 1 = 31$. The crosscorrelation values give, as expected, -1/31, 7/31, and -9/31 for (a), (b), and (c) respectively.

Since it is difficult and time consuming to find shift register feedback combinations that will yield Gold codes, tables of feedback combinations and irreducible polynomials have been generated [8] to make the task easier. Irreducible polynomials are another way of representing shift register feedback logic. For example the Gold code generator in Figure 2.5 may be represented by:

$$\begin{aligned} Q &= X^5 + X^3 + 1 \\ Q' &= X^5 + X^4 + X^3 + X^2 + 1 \end{aligned} \tag{2.5}$$

where the value of the exponents corresponds to the feedback taps that will be modulo-2 added.

Upon reviewing the properties of Gold codes, the stage is set to discuss the type of SS modulation techniques.

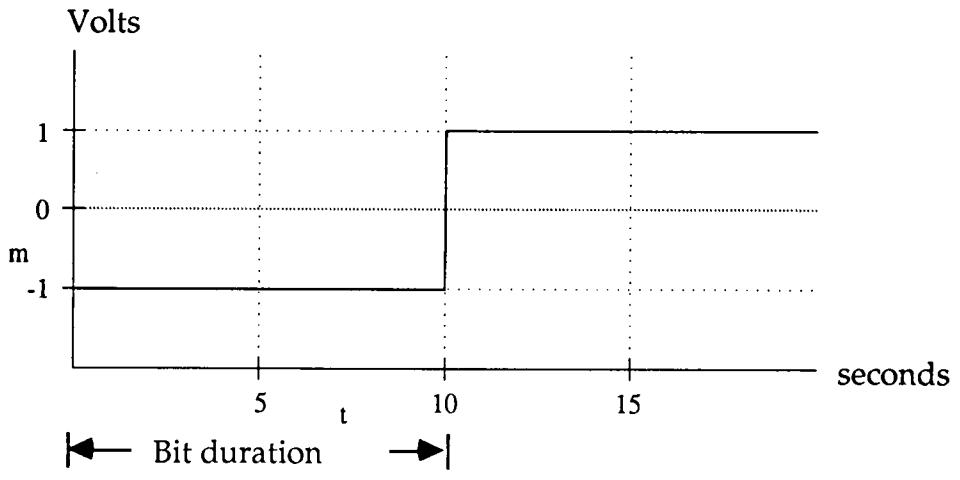
2.4 Direct Sequence Spread Spectrum

In DS/SS a carrier wave is first modulated by a digital message signal, $m(t)$, and subsequently multiplied by a high bit rate code sequence, $u(t)$. For every message bit a number of code *chips* are sent which result in the spreading of the transmitted signal bandwidth. Figure 2.6 shows a message signal and a code signal with 10 chips per bit represented by non-return to zero (NRZ) pulses where the digit "1" is represented by +1 volts and "0" by -1 volts. This is not nearly the usual ratio of chips per bit of information in DS/SS; normally the ratio is on the order of a thousand, but was chosen for illustration purposes.

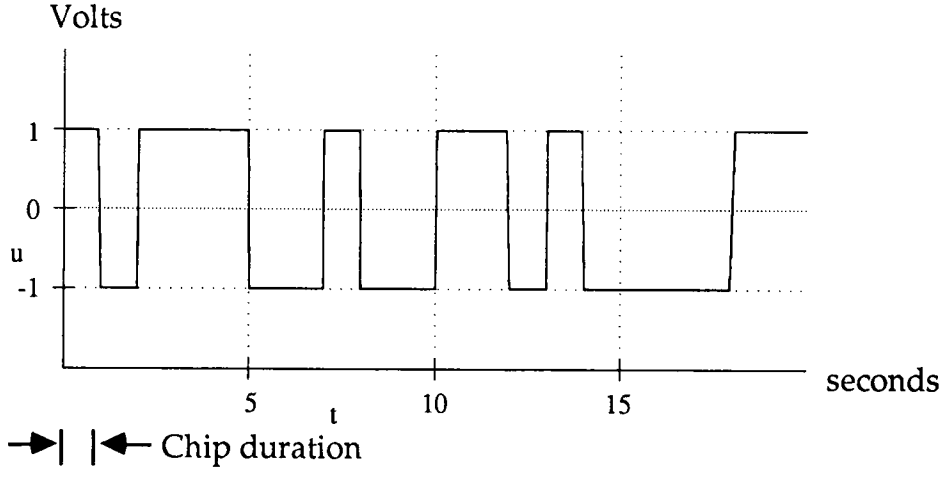
Assuming a sinusoidal carrier of amplitude A_c, carrier frequency f_c, and data phase modulation $\theta_m(t)$, a DS/SS modulated signal may be represented mathematically by

$$s(t) = A_c \cos[2\pi f_c t + \theta_m(t) + \theta_u(t)] \tag{2.1}$$

where $\theta_u(t)$ is the phase introduced by the code sequence. This parameter is rapidly varying, and as a consequence, it introduces high frequency components to the modulated carrier wave which result in the expansion of the transmitted signal bandwidth. A simplified block diagram of a DS/SS system with binary phase shift keying (BPSK) data modulation, is shown in Figure 2.7. The carrier is multiplied by an NRZ data pulse stream with bits encoded as shown in Figure 2.7. This is possible because BPSK changes the carrier phase carrier 180

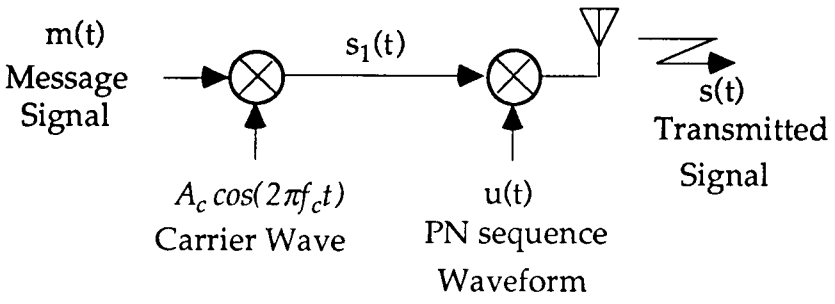


(a)

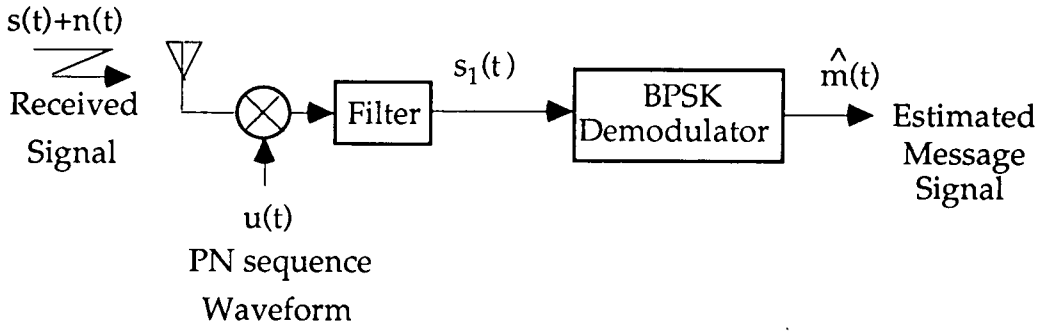


(b)

Figure 2.6 NRZ pulse waveform of (a) message signal (b) PN sequence.



(a)



(b)

Figure 2.7 DS/SS BPSK system (a) transmitter (b) receiver.

degrees for any "0" bit which is equivalent to multiplying by -1. Since the transmitted signal modulation format is phase modulation, the signal is normally coherently detected; that is, a phase reference is used in the detection process. For DS/SS systems, the signal can take on a number of phases for each chip duration, thus a receiver has to be able to achieve phase synchronization within a fraction of the chip duration. After synchronization is achieved, the receiver multiplies the detected signal with a code replica, $u(t)$, the same as the one which was used at the transmitter. This process despreads the bandwidth to its baseband bandwidth. The result is passed through a bandpass filter and then to a demodulator which reproduces the message signal. Note that the variable at the receiver has the symbol "^" because it represents an estimate of the transmitted message in the presence of noise.

Generally, in conventional systems there is a trade off between protection against detection or interception and resistance against interference because resistance to interference may be achieved by increasing the nominal transmitting power while resistance to detection or interception calls for a reduction of signal energy. In DS/SS, these qualities are complementary. Detection and interception resistance are possible because the total power of the message signal and the spread spectrum signal are the same. Therefore, the power spectral density of the transmitted signal is reduced by a factor of G_p, where G_p represents how many times the transmitted signal bandwidth is greater than the message signal and is equivalent to the ratio of the bit period T_b to the code chip period T_c or T_b / T_c. Since in typical systems this ratio is very large, on the order of a thousand, the transmitted power spectral density is very small, and in many cases, below the thermal noise floor of an intercept receiver [7]. Even under these circumstances, the signal is able to withstand interference because the PN sequence at the intended receiver despreads the signal

bandwidth to its baseband bandwidth while it spreads any interfering waveform arriving at the receiver the same way the signal was at the transmitter. A BPF removes the interference spectrum which does not overlap the signal spectrum. This process is shown graphically in Figure 2.8.

2.5 Frequency Hopping Spread Spectrum

Frequency hopping spread spectrum (FH/SS) modulation is achieved by randomly shifting the baseband bandwidth over a set of frequencies determined by a PN sequence. The sequence of bits generated by the PN generator are grouped into digital words which in turn drive a frequency synthesizer to produce a particular transmission frequency. The length of the digital words is determined by the frequency separation required between two consecutive hops and the total spread spectrum bandwidth required. For example, if a bandwidth of 800 MHz is required with a frequency separation between two hop frequencies of 8 kHz, then it will require at least 800 MHz/8 kHz hopping frequencies which translates to a word length of $\lceil \log_2(10000) \rceil = 17$ chips where $\lceil\ \rceil$ denotes the greatest integer function. Figure 2.9 is an illustration of a frequency synthesizer which selects frequencies in accordance with the three words produced by the PN code. The largest value corresponds to the word 111 and the frequency step size is 100 Hz.

In Figure 2.9, only eight hopping frequencies are available; actual systems employ multiple hopping frequencies which occupy bandwidths on the order of several gigahertz [6]. This is bigger than the possible band that can be implemented with DS/SS systems. It seems to appear then, that an FH/SS system is better than a DS/SS for protecting against interference or detection. However, at any given hop, the bandwidth occupied is the same as the conventional signal bandwidth; thus a jammer can induce some degradation by

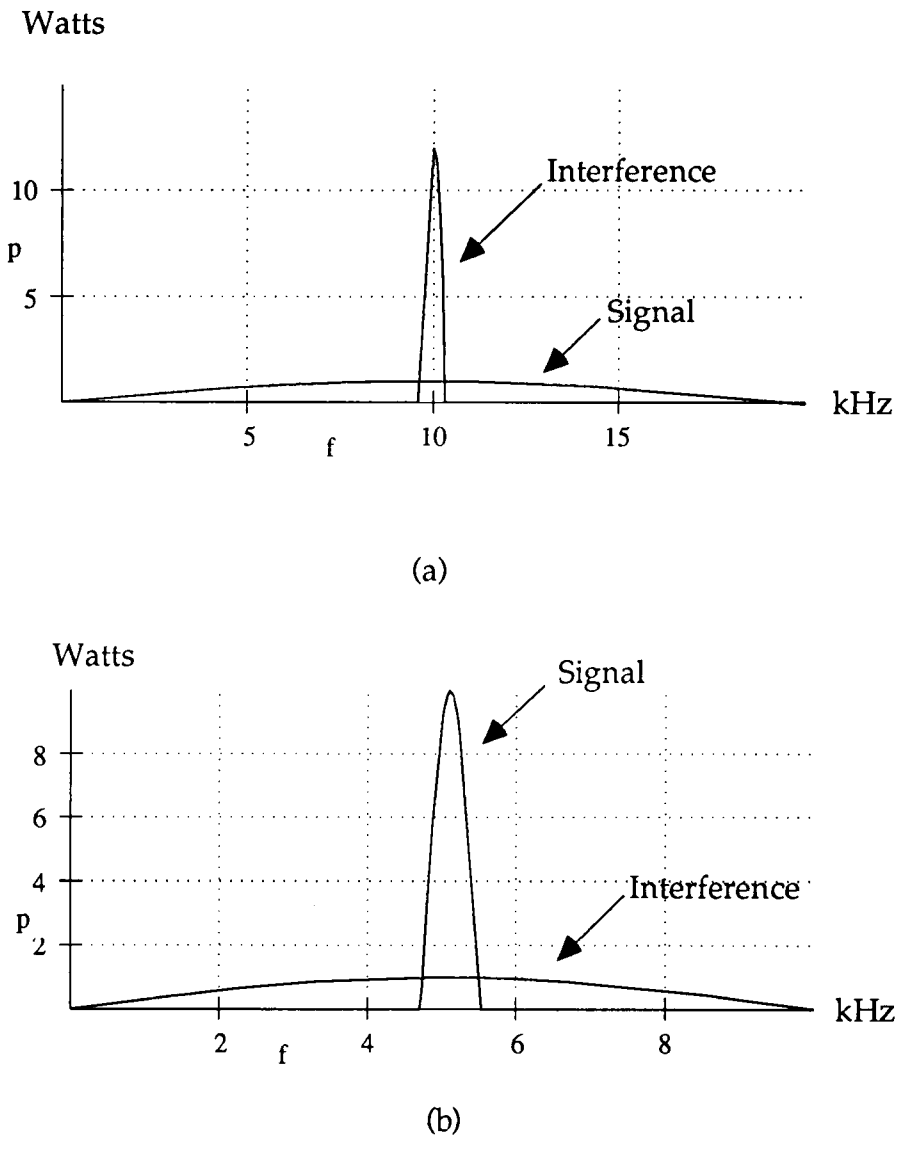


Figure 2.8 Spectra of desired signal and interference (a) receiver input (b) despreading demodulator output.

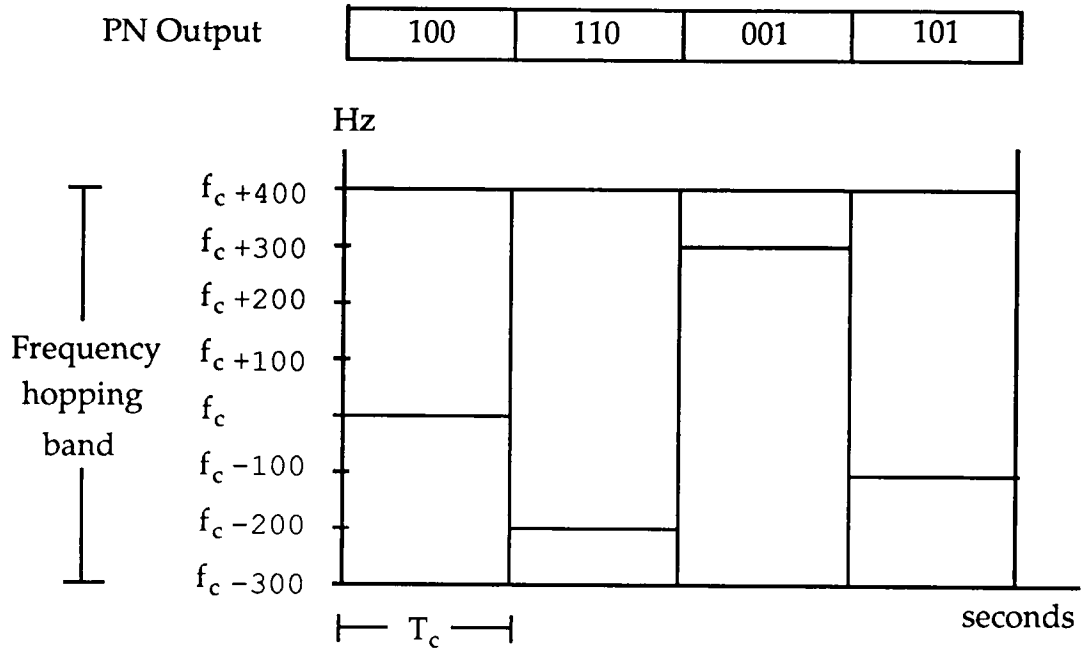


Figure 2.9 Frequency synthesizer output for four different 3-bit words.

jamming only a few frequency bands. Furthermore, a narrowband receiver may be able to detect the presence of a hopper and extract some of it features. This type of impairment is usually minimal. For example, a system employing a million independent hopping frequencies and a jamming signal with a bandwidth 10 times the message bandwidth will have about a 10^{-5} probability of being in the same band and degrading the message signal. The same probability will exist for an intercept receiver to detect a hop. So FH/SS offers great anti-jam protection [9], and while not as good as DS/SS, it still offers fairly good protection against signal interception and detection. Further aspects of frequency hop systems will be covered in the following chapters.

2.6 Other Spread Spectrum Techniques

The other fundamental spread spectrum modulation technique is *time hopping* (TH) which transmits data at instantaneous and variable time intervals. The message period, T, is divided into time subintervals of duration τ. For each message, a time subinterval is selected in accordance with a PN sequence generator in a manner similar to the case of hopping frequencies in FH/SS systems. All figures used to illustrate FH/SS systems may be used as references for TH/SS by substituting frequency with time and frequency synthesizers with time logic circuitry.

TH/SS is usually used in conjunction with DS/SS or FH/SS systems, thus it is not given a complete treatment here. There are also several hybrid systems in use in order to create yet more SS signals. These include hybrid DS/FH, FH/TH, DS/FH/TH and any other combination of the three.

2.7 Spread Spectrum and CDMA

SS systems have the desirable properties of interference rejection and protection against interception and detection. It would usually be very inefficient to use such a large bandwidth given the scarce RF spectrum. This problem may be treated by incorporating CDMA allowing a large number of users simultaneous use of the same frequency band. This occurs at the expense of some small but incremental mutual interference as the number of users increases. This is possible because each user can be assigned a unique spreading code so that an intended receiver will pick up only that signal to which it is matched; all other signals are treated as noise. The amount of mutual interference can be reduced by carefully selecting nearly orthogonal codes for the various users in the communication environment. The number of users that a system can support

depends on the amount of interference tolerable. For example, a system that only transmits voice may accept bit error rates (BER) of the order of 10^{-3}, while a digital data system with a BER requirement of 10^{-5} may be less tolerant of a large number of users.

Various commercial applications using spread spectrum require CDMA, such as the highly contested infant wireless communication services called personal communication networks (PCNs) [6], which provide communication access regardless of location. CDMA can be advantageous in this domain because it appears to offer greater capacity levels in terms of number of users per cell -- a cellular architecture is assumed much like the current cellular telephone systems -- than the other multiple access techniques (namely frequency division multiple access (FDMA) or time division multiple access (TDMA) [10] where signals are assigned non-interfering frequencies or time slots). In this work FH/CDMA is being proposed for a radio network in a factory environment. The following chapters will expand this concept more.

Chapter 3

Indoor Radio Propagation Characteristics

3.1 Introduction

The indoor radio propagation environment is very complex. Generally, the signal path between transmitter and receiver is blocked by walls, office partitions, ceilings, and other obstacles. As a result, multiple reflected copies of the same information arrive at the receiver at different times and at different power levels. This phenomenon is known as multipath fading. Multipath fading is a great problem for radio communication because it is a cause of intersymbol interference which severely limits the achievable bit rates in the indoor environment. In addition instantaneous fading or shadowing due to the movement of people or objects and local movement of terminals add more trouble to the already complex environment. Figure 3.1 shows a multi-ray model for a system with its transmitter in one room and its receiver in another room. Several possible paths for the transmitted signal are indicated to illustrate the complexity of the indoor propagation environment.

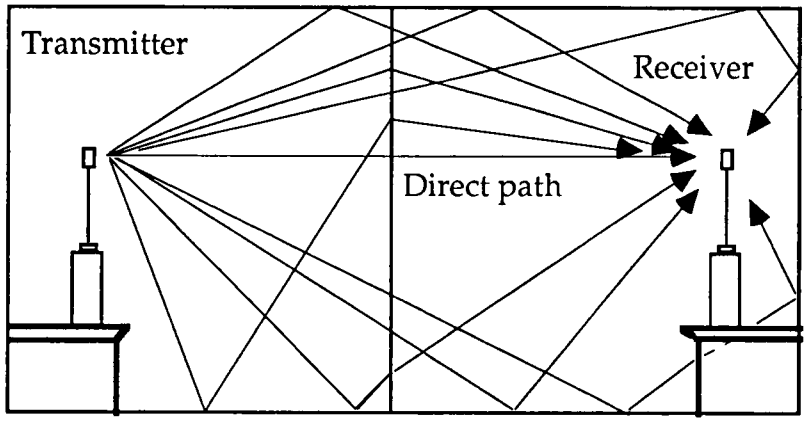


Figure 3.1 Multi-ray propagation model

The severity of the multipath fading depends on whether there is a direct signal path between a transmitter and a receiver. For example, a system confined to a room with no partitions will have a direct optical link between transmitter and receiver and thus less power attenuation than one which is operating in a partitioned room of the same size [11]. Thus two general categories may be devised to characterize radio wave propagation within buildings: line-of-site (LOS), if there is a direct signal path between transmitter and receiver, and obstructed-line-of-site (OLOS), for the absence of such a path.

A deterministic model for indoor radio propagation is virtually impossible to develop because the number of potential paths is too large and varies considerably as transmitters and receivers are relocated within a building. Therefore, indoor radio propagation is modeled statistically using the results of various measurements done at field site locations. This chapter will use such experimental field measurements as a model for different propagation scenarios.

3.2 Multipath Propagation Model

As stated earlier, a purely deterministic model for indoor radio propagation is very difficult to develop. However, propagation measurement results from different indoor environments suggest that a statistical model for multipath fading based on the discrete complex impulse response, $h(t)$, of the indoor channel represented by:

$$h(t) = \sum_k \alpha_k \delta(t - \tau_k) e^{j\theta_k} \tag{3.1}$$

where k is the path index; α_k is the amplitude of the pulse; $\delta(t - \tau_k)$ is the Dirac delta function; τ_k is the path delay associated with the k-th path; and θ_k

represents a phase shift induced by the reflection coefficient of scatterers. Since some of the energy of the incoming signal is reflected off obstacles in the signal path, the signal cannot maintain a straight line course -- see Figure 3.1. As a result, there is a change in direction every time a signal path intersects an object which induces a different phase angle. The phase angles induced by the obstacles in the signal path θ_k are assumed to be statistically independent random variables with uniform distribution in the interval $[0, 2\pi]$.

The τ_k and α_k have more complex statistics. Some models, as in [12, 13], assume that the τ_k are statistically independent variables and uniformly distributed in the interval $[0, T]$, where T is the pulse duration. Other models assume, as do the ones in [14, 15], that the arrival rate forms a complex Poisson process in which the signals arrive in clusters. The clusters are groups of rays that arrive within few nanoseconds of each other. In this model, all the clusters that arrive in a given receiver site are averaged to form a mean cluster rate Λ and the individual rate within a cluster are also averaged to form a mean arrival rate of λ. However, this model is not general enough to fit all situations because the clusters are assumed to be formed from building structures such as walls; for factory environments that is generally not the case [14]. The received signals in factories consist of multiple scattering components of the incoming signal bouncing from a large amount of equipment usually present in the factory.

The statistics of α_k are better defined. For LOS situations, a significant part of the received signal power is due to one particular path with an unobstructed view between the transmitter and receiver. The overall channel is characterized by a strong or main component in addition to the multipath components which may be the result of reflections off the floor, walls, or ceiling of the indoor measurement space or the movement of people and inventory within the building . A representative indoor environment in which this situation

may occur is in supermarkets where there may be at least one direct path between transmitter and receiver and the aisles act as wave guides for radio propagation. This model is represented by a Rician amplitude fading envelope. The Rician probability density function (pdf) is given by the following:

$$p_x(x) = \frac{x}{\sigma_k^2} e^{-\left(x^2+A^2\right)/2\sigma_k^2} \; I_0\left(A_x / \sigma_k^2\right); \quad 0 \le x < \infty, \; A \ge 0 \tag{3.2}$$

where σ_k^2 is the variance of the random multipath. The parameter signal amplitude of the dominant path is expressed by A, and $I_0\left(\frac{A_x}{\sigma_k^2}\right)$ is the modified Bessel function of the first kind and zero order . A graphical representation of a Rician pdf is shown in Figure 3.2.

For an OLOS indoor environment, the signal has to pass through obstacles, thus causing severe degradation of the transmitted signal. Path loss as severe as 20 to 30 dB have been reported in [16]. A typical multi-story office building in which there are many partitions to accommodate different offices, may have a transmitter and receiver separated by a number of walls or floors. Various experimental results show that the path amplitudes α_k form a Rayleigh distribution [9,10,11]. The Rayleigh pdf may be expressed mathematically as follows:

$$p_x(x) = \frac{x}{\sigma_k^2} e^{-\left(x^2+A^2\right)/2\sigma_k^2} \; ; \quad 0 \le x < \infty, \; A \ge 0 \tag{3.3}$$

A graphical representation of the pdf is shown in Figure 3.3. In observing both the Rician and the Rayleigh amplitudes models, it is obvious that the Rician amplitude model is more dispersive than the Rayleigh, as demonstrated by the width of their curves. Note that both pdfs have a variance of σ_k^2=1 and are

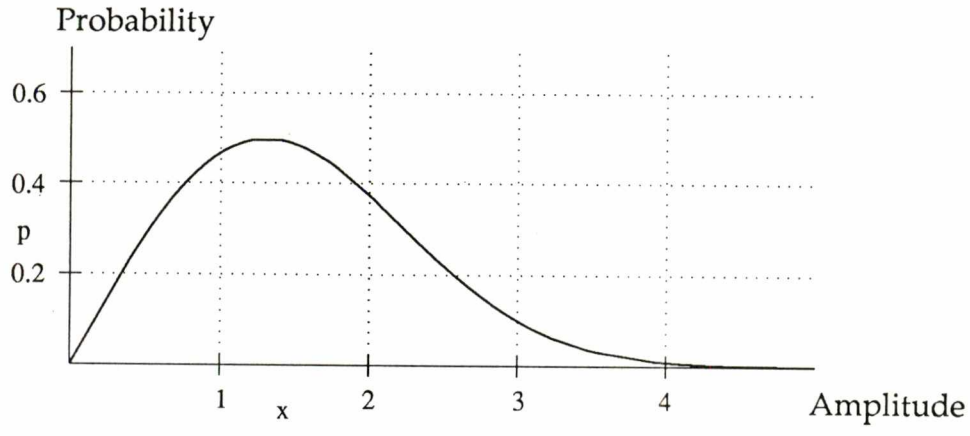


Figure 3.2 Rician pdf.

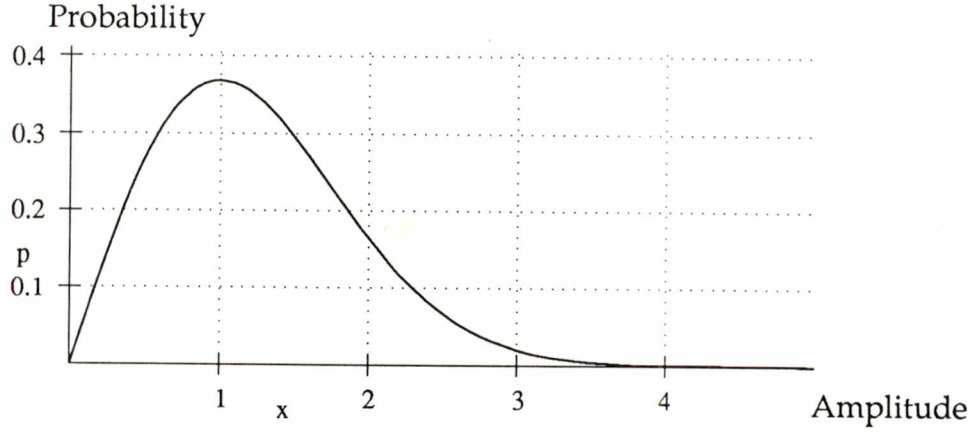


Figure 3.3 Rayleigh pdf.

plotted on the same scale axis. For example, in Figure 3.3 the probability that the amplitude will fall in a differential interval around the number 1 is about 0.35 while the probability that the amplitude will fall in a differential interval about the number 4 is practically zero. This is an indication of the severity of Rayleigh fading with respect to the Rician; using the same numbers considered in the example above the probabilities are 0.45 and .02 respectively. There are other amplitude models such as the Lognormal, Weibull, Nakagami-*m*, and Susuki, but the aforementioned models appear to fit most of the propagation indoor environments [12]. Therefore, indoor radio channels are generally modeled by either a Rayleigh or a Rician fading model.

3.3 Indoor Channel Propagation Measurements

As stated earlier, in order to characterize the indoor radio environment, field site measurements have to be taken. The statistics of this measurement data depend on the architecture of the building; that is, the number of walls between transmitter and receiver, the size of the indoor space, the number of floors in the building as well as the construction material. The construction material is very important. For example, a building made up of metal walls like some warehouses will offer considerable resistance against diffusion for a signal to pass through, but it will provide a lot of scattering components due to the highly reflective surfaces. In contrast, a residential building with interior paper walls allows signals to propagate much easier through the walls than bounce or reflect off them. All of these subtleties are what make the indoor channel difficult to model.

The indoor radio propagation measurements are based on the statistics of the received power and the multipath delay characteristics. These statistics are defined by the RMS delay spread σ and the mean excess delay $\bar{\tau}$. The mean

excess delay is the first moment of the power delay spectrum G and the RMS delay spread is the square root of the second moment of the power delay spectrum . The power delay spectrum is the sum of all the multipath power gains. Mathematically these parameters may be expressed as follows [15]:

$$G = \sum_k \alpha_k^2 \tag{3.4}$$

$$\bar{\tau} = \frac{\sum_k \alpha_k^2 \tau_k}{G} \tag{3.5}$$

$$\sigma = \sqrt{\overline{\tau^2} - (\bar{\tau})^2} \tag{3.6}$$

$$\overline{\tau^2} = \frac{\sum_k \alpha_k^2 \tau_k^2}{G} \tag{3.8}$$

Depending on the frequency band used, emphasis may be given to either the received power or the multipath delay. For narrowband signals, such as the cordless phone which operates in the 46-49 megahertz (MHz) frequency band, measurements are based mostly on the statistics of the received power, while for broadband measurements, the multipath delay characteristic of the channel is of equal importance [3].

3.3.1 Narrowband Measurements

In narrowband measurements, the information extracted is the relation between the multipath received power and the distance from transmitter to receiver [3]. The multipath received power ,$G(d)$, has been found to be inversely proportional to distance, d, from transmitter to receiver.

This relation may be expressed mathematically as below:

$$G(d) \propto d^{-\alpha} \tag{3.4}$$

where α is the attenuation factor. For free space α=2, but for indoor environments, it can fluctuate from less than 2 to as high as 6. Lower values of α (compared to free space) are obtained in situations where measurements are taken in hallways or aisles that tend to enhance propagation and act more like wave guides. On the other hand, higher values of α result from signal blockage by obstacles in the path from transmitter to receiver. Thus, the construction material as well as the number of obstacles in the way of the shortest path between transmitter and receiver will play a major role in the value of the attenuation factor. For example, in a building with metal partitions, attenuation factors close to 6 are not uncommon [16]. Since narrowband applications are restricted to cordless phones and low speed data transmission, wideband propagation measurements, which will be required to model high bit rate data transmission for wireless indoor networks envisioned for the future, have received more treatment in the literature in recent years. The discussion presented next will be based on wideband channel measurements.

3.3.2 Wideband Measurements

Wideband communications uses narrow pulses in the time domain which translate into large frequency content in the frequency domain. If the duration of the signal pulse is several times smaller than the shortest and longest propagation delays between transmitter and receiver, the receiver will observe several isolated pulses for each transmitted pulse. Therefore wideband propagation measurements deal primarily with multipath propagation and related statistics [3]. For example, Figure 3.4 shows a multipath profile measured at 910 MHz at a location on a manufacturing floor. The delay between the first

and second pulse is about 7 nanoseconds (ns), which is associated with a 2.1 meter (m) difference between the distance traveled by the first path and that traveled by the second (note that the distance relation is determined by the speed of propagation, which is the same as the speed of light $3 \cdot 10^8$ m/s). Note that the second arriving pulse has a larger amplitude than the first. This may be due to constructive interference involving a number of signals arriving at the receiver site at the same time with small phase differences thus resulting in the near coherent addition of the signal amplitudes.

To obtain a complete multipath delay profile, several measurements of the RMS delay spread and multipath power fluctuation are taken from different locations in the indoor environment under consideration. The result of these measurements is plotted and used to characterized the indoor environment. Figure 3.5 shows the variation of the RMS delay spread over a partitioned indoor radio channel for a 3 ns pulse transmitted at 910 MHz. Measurements were done at the Atwater Kent Laboratories at the Worcester Polytechnic Institute; the LOS consisted of all measurements inside the electronic laboratory; the OLOS1 comprised all measurements with the transmitter separated by the receiver by one wall and some window glass; and for the OLOS2, the transmitter and receiver were separated by at least two walls [14]. RMS delays range from 4-16 ns for LOS and 10-38 ns. The relatively short delays are due to the distance between the transmitter and receiver, which was limited to between 7 and 20 m. Figure 3.6 shows a power attenuation difference of a 7.5 dB between the case of LOS and the OLOS2. The design of indoor radio propagation is highly dependent on the architecture, size of the indoor environment under consideration, and the construction material. The architecture is important because it determines the number of obstructions in the signal path between the transmitter and receiver, which governs the level of signal fading.

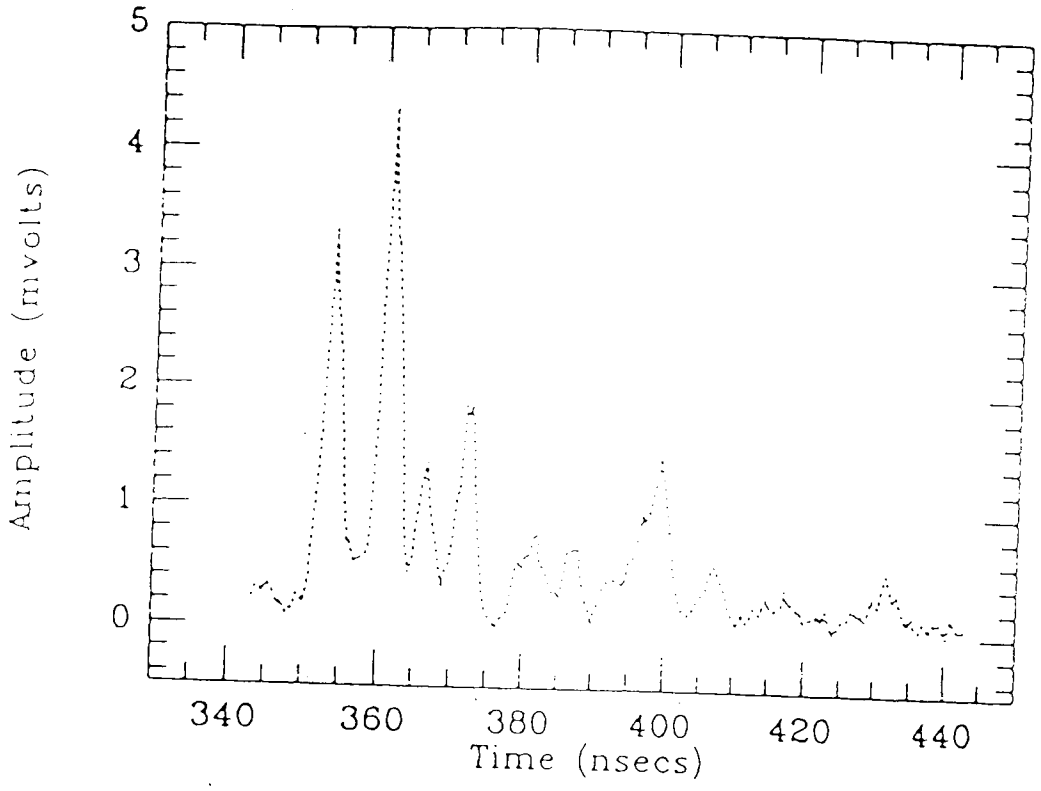


Figure 3.4 Multipath delay profile from one location on a manufacturing floor.

Reprinted from: Rajamani Ganesh and Kaveh Pahlavan, " On the Modeling of Fading Multipath Indoor Radio Channels", IEEE Globecom, Vol. 3, pp. 1346-1349, 1989, © 1989 IEEE.

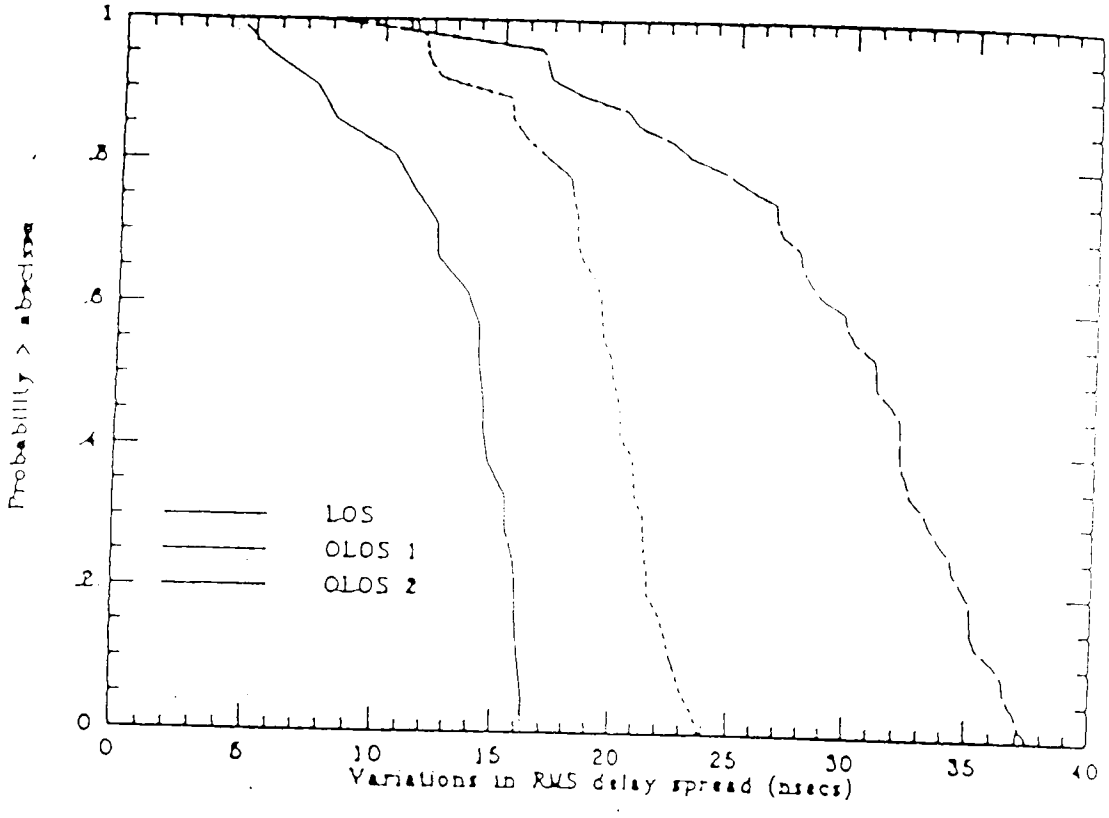


Figure 3.5 Variation of RMS delay spread (ns)

Reprinted from: Rajamni Ganesh and Kaveh Pahlavan, "Statistical Characterization of a Partitioned Indoor Radio Channel", IEEE International Communication Conference pp. 1252-1256, 1992, © 1992 IEEE.

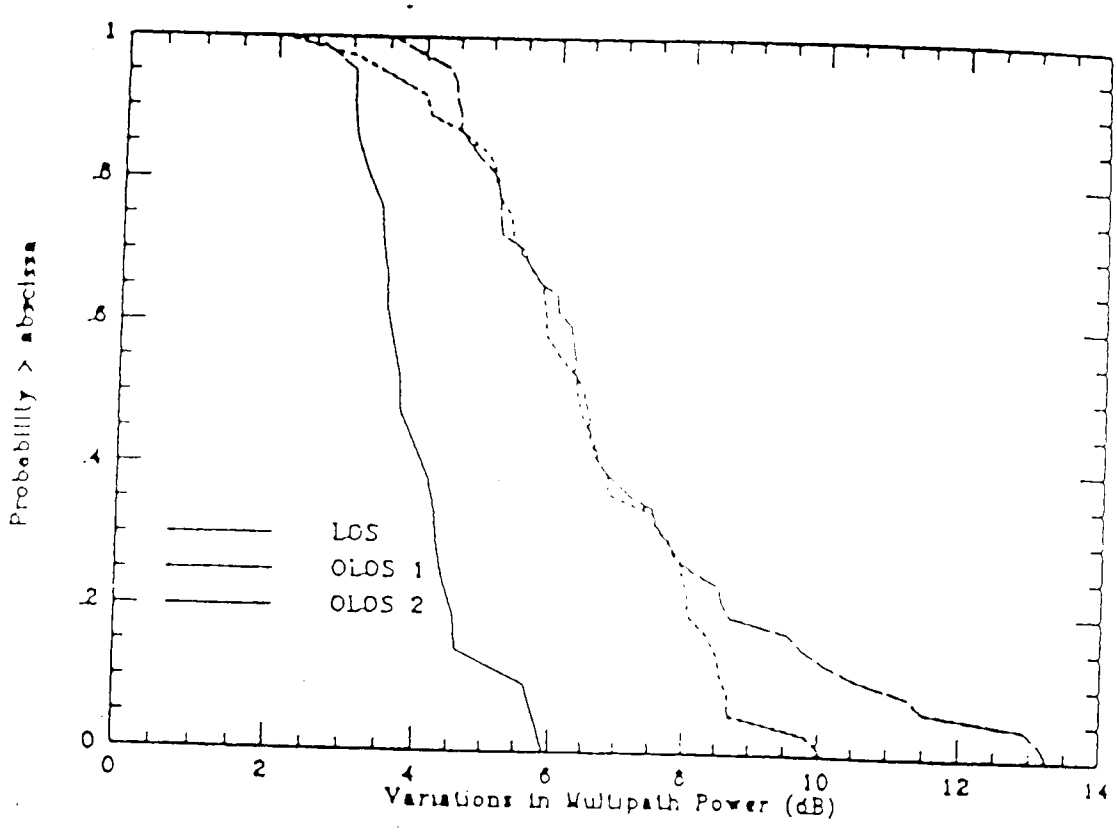


Figure 3.6 Variation of multipath power (dB)

Reprinted from: Rajamni Ganesh and Kaveh Pahlavan, "Statistical Characterization of a Partitioned Indoor Radio Channel", IEEE International communication conference pp. 1252-1256, 1992, © 1992 IEEE.

In addition, the size of the building contributes greatly to the RMS delay spread. All these factors are what make absolutely necessary the measurement of the indoor radio propagation characteristics to design wireless indoor radio systems [3]. However, as stated earlier, statistical channel models of the indoor radio propagation characteristics may be used for simulation purposes. Therefore, the wireless indoor radio system simulation developed in the next chapter was designed around a Rayleigh fading channel model which is a statistical model of the indoor radio propagation.

Chapter 4

FH/BFSK/CDMA Simulation Program for the Factory Environment

In Chapters 2 and 3 general concepts about SS techniques and characteristics of the indoor radio channel were developed. In this chapter, the anti-multipath fading characteristics of SS techniques will be tested by developing a simulated model for an FH/BFSK/CDMA indoor radio network. FH/BFSK/CDMA stems from the fact that the system uses many transmission or hop frequencies, FH; uses two frequencies to encode either a binary one or zero, BFSK; and provides multiple access via PN codes, CDMA. Schematic representations of the components of the system (transmitter, channel, and receiver) will be developed accompanied by their computer simulated structures.

The computer simulation is done with the Laboratory Virtual Instrument Engineering Workbench (LabVIEW) which is a graphical programming language that uses virtual instruments (VIs) to perform computations, to simulate physical instruments, and to perform any kind of task that can be done by conventional programming, like C, FORTRAN,...etc [12]. The virtual instruments are represented by icons and are connected together in a block diagram that specifies the control flow of the data -- like the source code in conventional programming. LabVIEW is a useful programming tool for design applications because other than the block diagram which provides a visual representation of the design application, it offers a front panel where inputs may be manipulated interactively and outputs may be observed in graphical, array, or tabulated forms. The advantages of using LabVIEW in simulating communication systems will

become apparent as detailed explanations of the system under consideration are given in subsequent sections.

4.1 System Design Considerations

The system will be operating in a factory environment and in the worst case scenario possible; that is, the channel will be modeled based on the OLOS topography which fits a multipath Rayleigh fading channel (see Section 3.2). This is done to ensure that the performance level obtained is the worst possible. It will be assumed that the bit rate in the indoor radio channel is much faster than the fading rate, so that the random parameters associated with the indoor radio channel stay basically invariant over one bit period, clearing the way to evaluate the statistics of the channel on a per bit duration , T, basis. Therefore, the paths considered are those with delays restricted to the interval $[0, T]$ and random phases uniformly distributed in the interval $[0, 2\pi]$.

Since the system is a multiple access system, it is important to set some guidelines about users' access and operations:

- Users access the network asynchronously; that is, there is no network control. Any user can access the network at any time.
- All users transmit at the same power levels, so that no advantage is given to any user to overpower the others.
- The transmitter and receiver of a given link are assumed to be in perfect synchronization at the code level, so that there is no uncertainty as to when bits start and stop at the receiver.

The system may operate in the Slow Frequency Hopping (SFH) mode or in the Fast Frequency Hopping (FFH) mode. The SFH mode occurs when the bit rate of the system is greater than the hopping rate and the opposite is true in the

FFH mode. The bit rate is the number of message bits transmitted per second and the hopping rate is the number of different transmission frequencies per bit or bits of information. For example a system that employs a different frequency for every five bits will be described as an SFH system while one that transmits every bit at five different frequencies will be an FFH system. The merit of both modes will be discussed in the next chapter.

The system will be tested based on BER performance given a certain signal to interference density ratio. Thus, the BER of the system depends on the combined effects of the background or thermal noise which is modeled as Average White Gaussian Noise (AWGN), the multipath fading, and the multiple access interference (MAI). The effects of all these disturbances should be included in the design if realistic performance results are to be obtained.

Based on the design considerations outlined above, an FH/BFSK/CDMA indoor radio network is simulated. Figure 4.1 is the general block diagram on which the simulation is based. Note that the link of interest is the one that has the direct path; all other links represent interference. The MAI, due to other users and their multipath fading effect, are represented by the upper branch block labeled *K - 1 other users* and their channels. It was concluded in [5, 6] that MAI is the most devastating type of interference because each user adds to the multipath fading degradation by increasing the number of signal paths that reaches the receiver. This increases inter-symbol interference (ISI) and thus performance degradation. The degradation induced by the AWGN depends on the thermal noise of the indoor environment which is fixed no matter how many users are added. Therefore in some studies this is neglected but it is modeled as part of the channel.

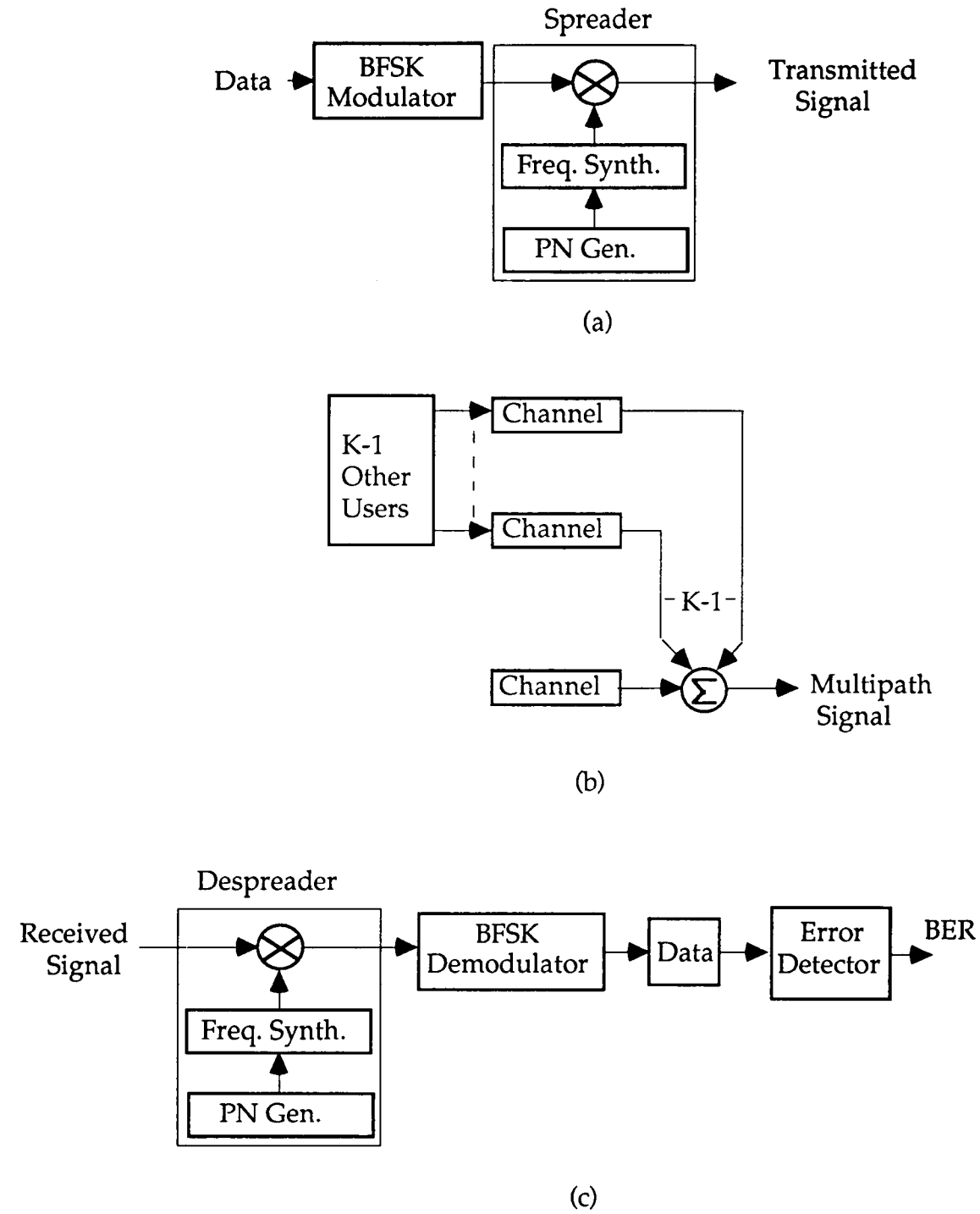


Figure 4.1 FH/BFSK/CDMA system (a) transmitter (b) channel (c) receiver.

4.2 System Simulation

The simulated system is a scaled down but faithful model of the actual system. The actual design parameters were used whenever possible, but due to memory limitations of the LabVIEW software system on the Macintosh IIx used, the following adjustments were made to ensure satisfactory operation:

1) Data bits are transmitted and detected one by one; that is, the data rate is normalized to 1 bps . By using a normalized value for the data rate, all operations are done sequentially on a bit by bit basis. This way, the system requires less memory but runs slower than if the operations were done in a group of bits.

2) The transmission or hopping frequencies are restricted to the interval from 1 to 800 Hz, again for memory considerations. For satisfactory results, LabVIEW requires a sampling rate of about five to ten times the highest frequency value. Thus, a frequency of 800 Hz requires about 800x5 or 4000 samples. Due to the size of the program the system was saturating at about 5000 samples. Although FH/SS operates at much higher frequencies, the transmission frequency range of 1 to 800 Hz does not hinder the simulation of the system. For example a system operating in the 900 MHz band and employing 100 different frequencies with frequency spacing of 4 MHz, may be simulated by a system employing 100 different frequencies with 1 Hz minimum frequency and frequency spacing of 4 Hz. This is possible because both systems will have the same G_p which is, in an FH/SS system, equivalent to the number of frequencies.

With these adjustments the stage is set to explain the simulation program. First, the integrated program which represents the actual system will be described. Then, the transmitter, channel, and receiver alone with their individual components will be described.

4.3 Simulation Program

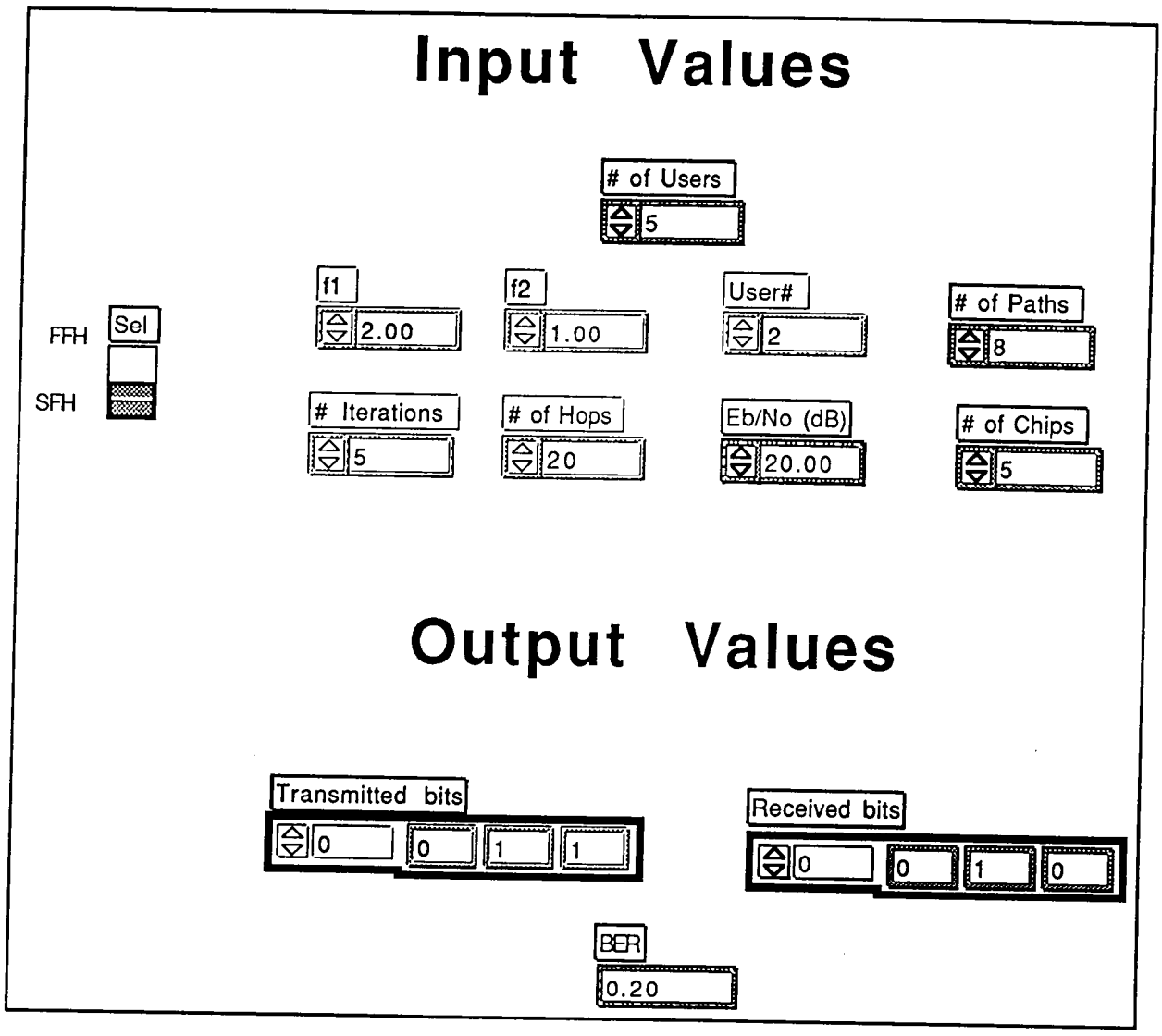
Figure 4.2 is the LabVIEW implementation of the FH/BFSK/CDMA system. On the front panel (Figure 4.2a), the following variables represent the input values. All input values may be set interactively by the operator of the program. Their definitions follow below:

- Sel -- selector switch; it allows for the selection of either FFH (*on* position) or SFH (*off* position).
- # of Users -- number of simultaneous transmissions, not to exceed twenty.
- f1 -- frequency that represents a binary one, it should be bigger than the frequency f2.
- f2 -- frequency that represents a binary zero, it should be less than f1.
- User # -- choice of the user to demodulate.
- # of Paths -- number of different paths between transmitter and receiver for the link of interest.
- # of iterations -- number of repetitions of the transmission process.
- # of Hops -- number of transmission frequencies, not to exceed 100.
- Eb/No -- signal to noise ratio.
- # of Chips -- the number of bits/hop for SFH or the number of hops/bit for FFH.

The output values are self-explanatory; they are the transmitted bits, the received bits, and the bit error rate BER.

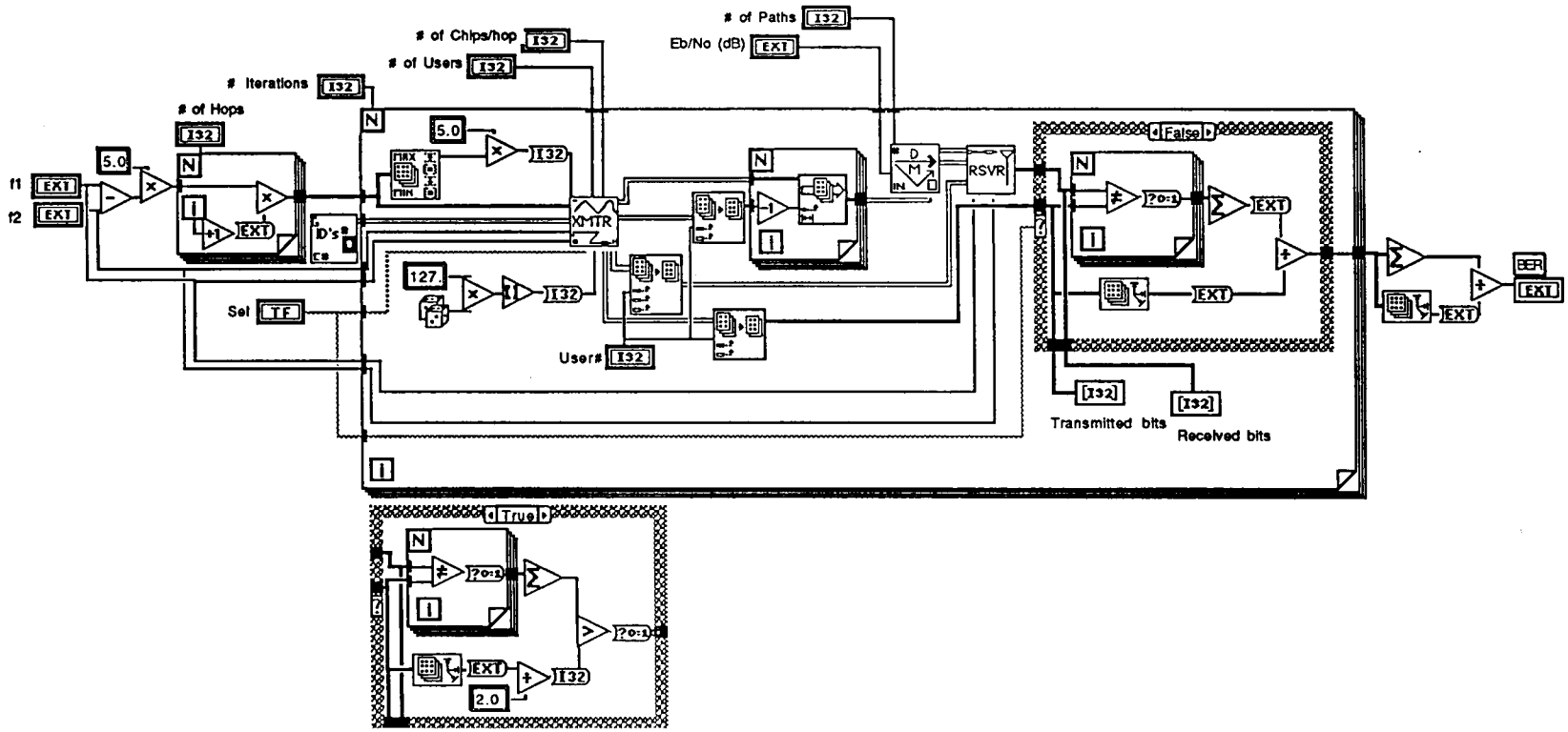
The block diagram (Figure 4.2b) represents the logic that governs the input values to give the output values of the program. The icons that resemble stacks of paper with an N in the upper left corner and i in the lower left corner are *for loops*. The N represents the number of times the operations

Front Panel



(a) Front Panel

Figure 4.2 FH/BFSK/CDMA System



(b) Block Diagram

Figure 4.2 (Continued)

within the loop are repeated and the i is the current index value for the loop; the index starts at zero.

The big for loop represents the heart of the program. The *# of Iterations* controls the number of times the operations within the loop are repeated. Within, the loop, basically all the iterated operations take place. The values calculated before the big for loop are values which remain the same throughout the transmission process. These values include: the transmission or hop frequencies and the PN codes. The transmission frequencies are created by the small for loop attached to *# of Hops*. This loop creates a set *# of Hops* transmission frequencies with frequency spacing of four times the difference between the two encoding frequencies. The PN codes come from a {7, 3} and a {7, 1} Gold code generator VI which is labeled by *ID's*.

Inside the big for loop, the transmitter VI represented by *XMTR* creates a *# of Users* simultaneous transmissions over the same frequency band to simulate the multiple access capability of the system. Since the operator of the system wants to listen to one user at a time, the Gold code of the user to be listened to, as well as its transmission time delays and transmitted bits are isolated with the index array function. The Gold code of the user is needed in order to keep track of its transmission frequencies; the delays are needed in order to set a reference delay of zero with respect to the other users; and the transmitted bits are needed to compare them with the detected bits for error calculations. The transmitted signal from the *XMTR* travels to the small for loop where the delays of the users are initialized with respect to the reference user (the user that the operator of the program wants to listen to). With this small adjustment, the signal is passed through the channel VI labeled D , above the straight arrow. This VI models the signal to noise ratio level E_b / N_0 and the number of paths between the transmitter and receiver *# Paths*. Then, the receiver follows. It is represented by

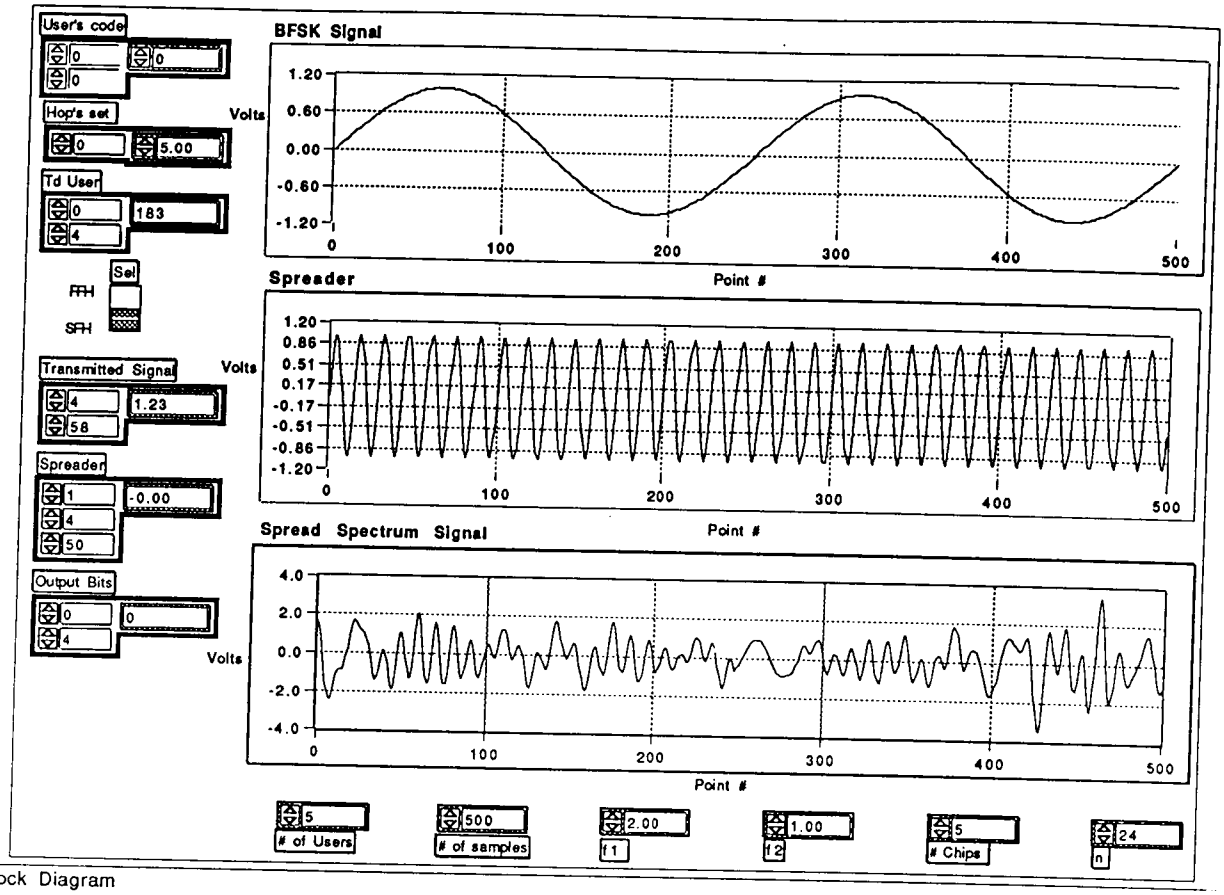
the *RSVR* VI. The last element in the big loop is a case structure. The case structure keeps track of the error for each iteration. The true condition of the structure determines the BER per iteration for FFH and the false case determines the BER for SFH. The BER for each iteration is added as shown by the summation operand at the right side of the loop, and the result of the sum is divided by the number of iterations to determine the BER of the system.

The following sections will describe the individual components that make up the simulation program. These components are known in LabVIEW as sub-VI's because they are subordinate to the main program. There are many built-in sub-VI's in the LabVIEW library but more may be created to perform more specific functions by the user. The sub-VI's discussed below are all user-created and are grouped along the line of the basic components in a communication link, that is transmitter, channel, and receiver.

4.3.1 Transmitter Sub-VI's

Figure 4.3 represents the front panel and block diagram of the transmitter. The purpose of this VI is to create the number of simultaneous transmissions specified by the *# of Users*. First, it takes a user's code and rotates the code by the number of spaces specified by the *n* array rotator sub-VI to ensure that the binary frequency words generated by *SPRD* sub-VI changes for each iteration. For each iteration a frequency word is transmitted for each user to determine the transmission frequency for that user from the hop set. The transmission frequency is mixed with the BFSK signal to produce a transmission signal for that user. The generated signal is given a random delay by the small loop inside the bigger loop. This process is repeated for each user and the results are added to simulate the effect of MAI. The transmitter is composed of the following sub-VI's:

Front Panel



Block Diagram

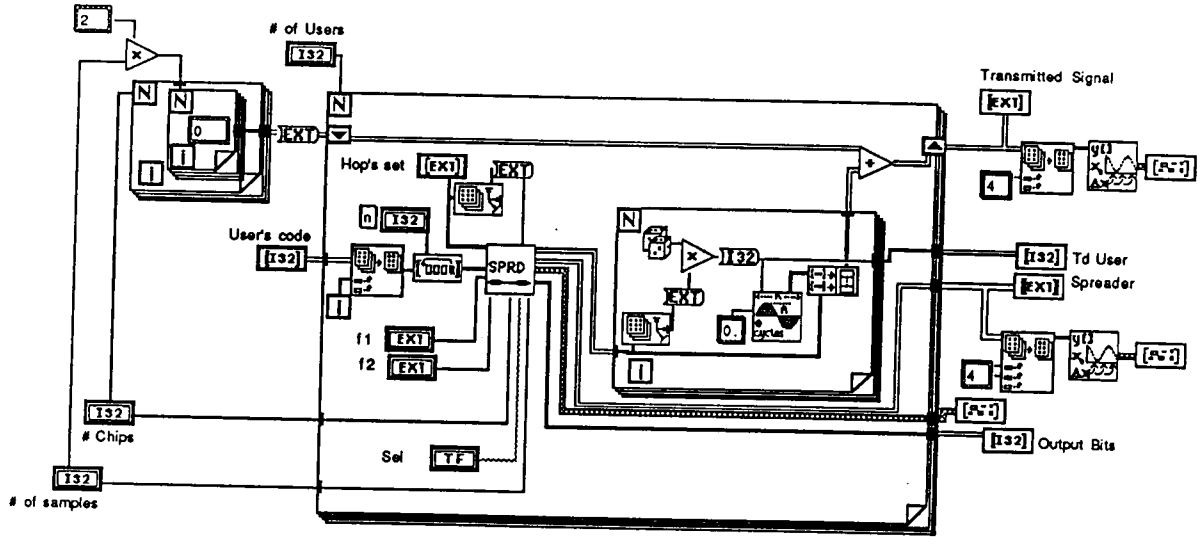


Figure 4.3 Transmitter VI

A. "BFSK" Encoder Sub-VI

The "BFSK" Encoder sub-VI shown in Figure 4.4 takes a set of binary random values consisting of ones and zeros and converts them to sinusoidal waves of random phase offsets and frequencies, f1 and f2, depending on whether a one or a zero was sent, respectively. The random phase offsets are limited to the interval [0, 2π]. The random bit generator is placed outside the loop to ensure that the bit generated is transmitted as many times as determined by the *# of Chips* and at different frequencies; this ensure a hopping rate larger than the bit rate, which is the case for FFH . SFH is similar; the only difference is that the bit generator is placed inside the loop so that the bit rate is larger than the hopping rate.

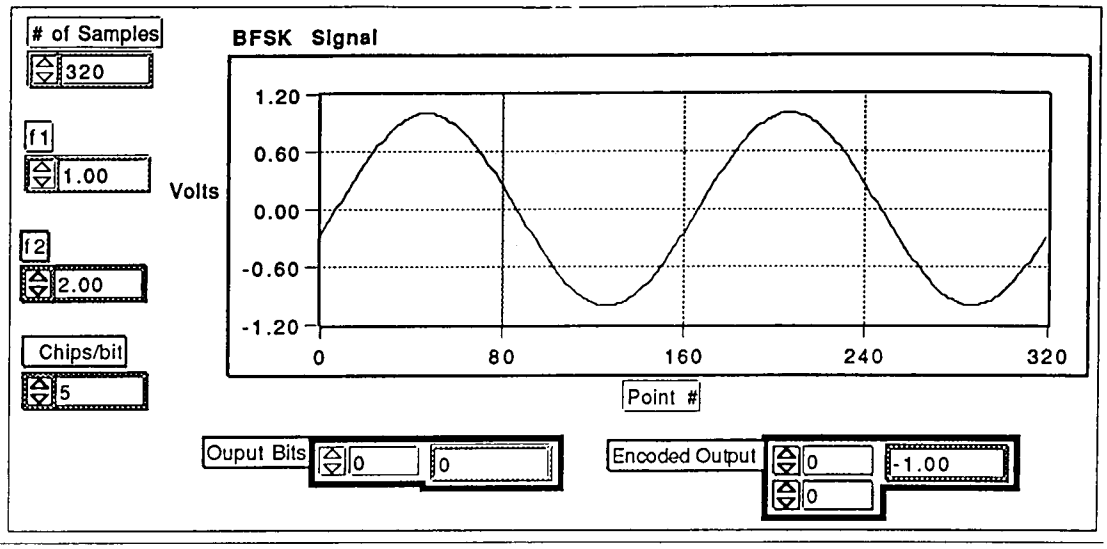
B. "Gold Code Generator" Sub-VI

The "Gold Code Generator" sub-VI as shown in Figure 4.5 represents a Gold code generator. It generates the user's PN codes to enable multiple access. These codes result from modulo-2 addition of a {7,3} and a {7,1} maximal length sequence. The designation of the sequences by two numbers in a bracket is one of many used to specify which output stages are modulo-2 added during the next clock pulse. This could have been expressed by the codes' irreducible polynomials in the same way with the numbers passing as exponents of the irreducible polynomial. Thus the two registers could have been described as:

$$\begin{aligned} Q &= X^7 + X^3 + 1 \\ Q' &= X^7 + X^1 + 1 \end{aligned} \tag{4.1}$$

where Q and Q' represent the LFSR's. The first LFSR, {7, 3}, is represented by notation R1 through R7. The output of the stages R3 and R7 are modulo-2 added, and the result is input to the register on the right side of the loop, which in turn,

Front Panel



Block Diagram

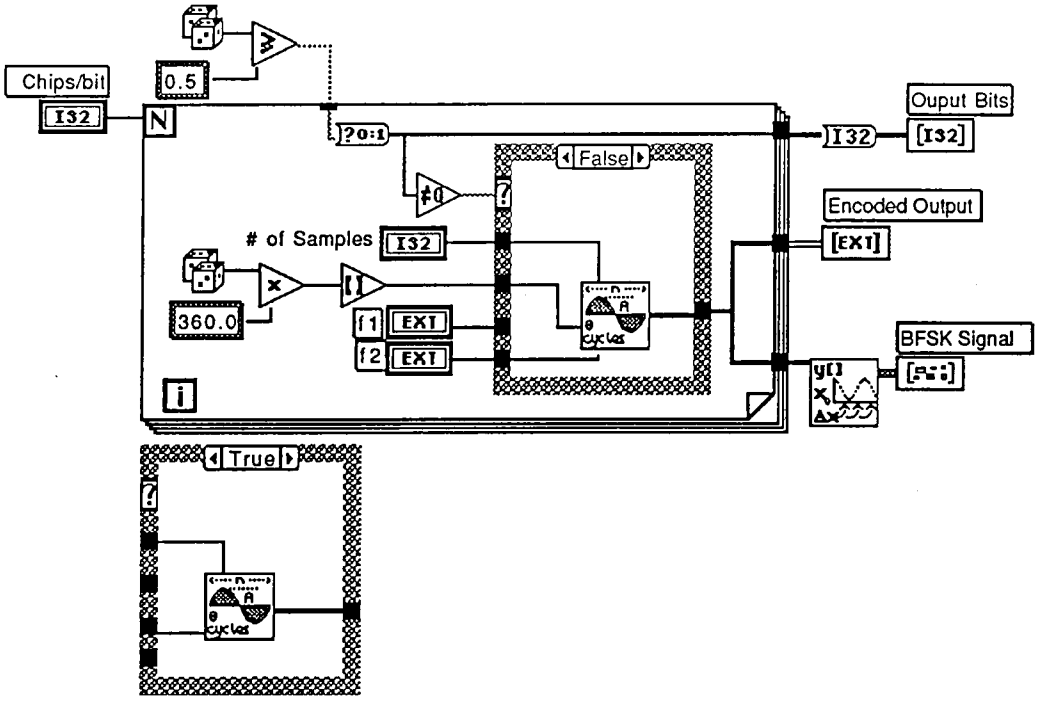
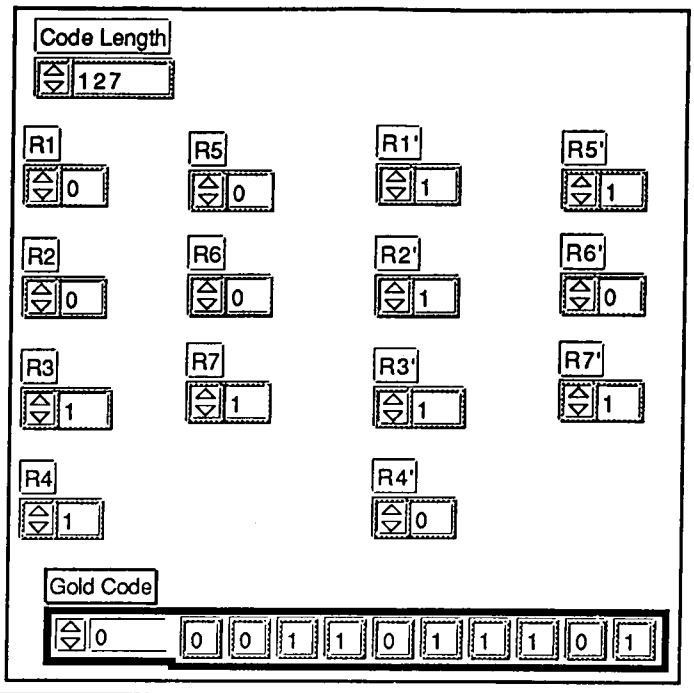


Figure 4.4 "BFSK" Encoder Sub-VI

Front Panel



Block Diagram

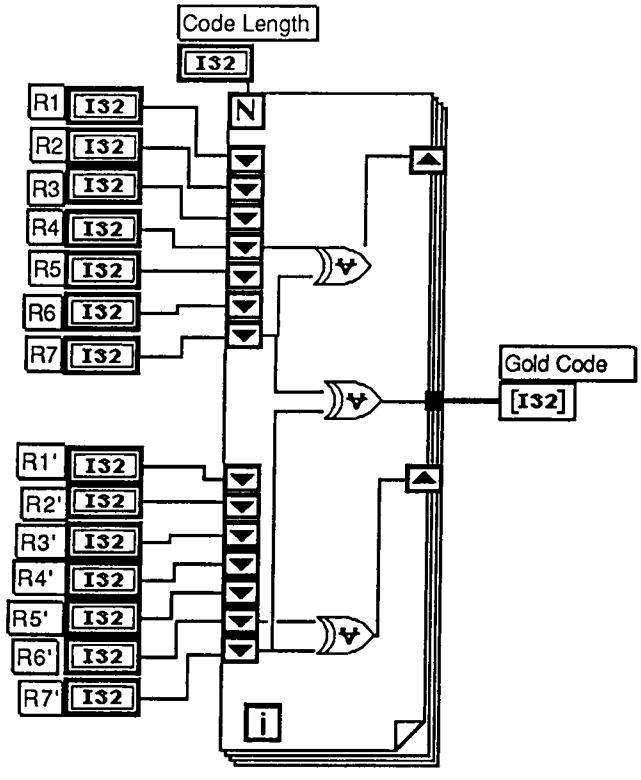


Figure 4.5 "Gold Code Generator" Sub-VI

feeds back the value to the first stage R1 during the next clock period. The direction of the arrows in the register diagram points the way data flows at the different stages of the LFSR circuit. That is, data flows from the register on the right side of the loop to R1, the value of R1 to R2, and so on to R7. The same process is repeated for the second LFSR , {7,1}, only here the modulo-2 addition is done on the registers R7' and R1'. Successive outputs of the two LFSR's are taken in the last stages, R7 and R7' of the registers, and they are modulo-2 added to produce a Gold code. A conceptual block diagram of the sub-VI is represented in Figure 4.6 to aid in visualizing the LabVIEW implementation of the Gold code.

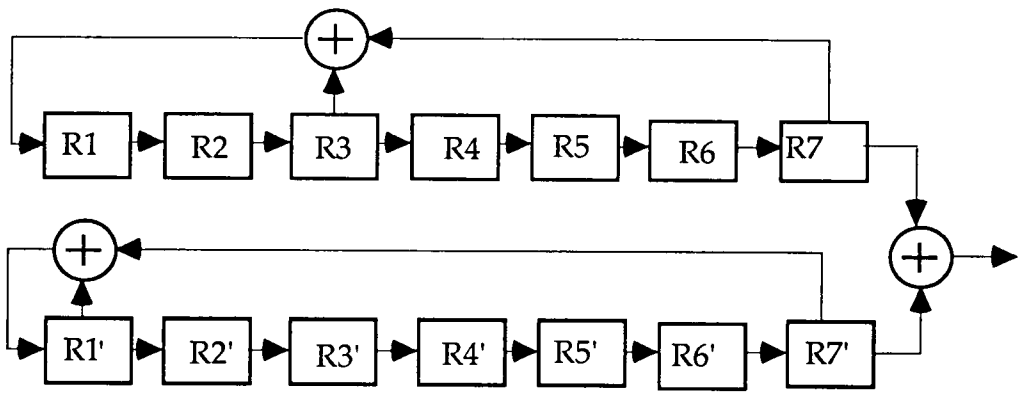


Figure 4.6 {7,3} and {7,1} m-length Gold code generator

Thus, as expressed by Equations (2.3) and (2.4), the possible values for the cross-correlations of the simulated Gold code yield -17/127, -1/127 and +15/127. In order to get these low cross-correlation values, the initial condition of the registers should be chosen very carefully. First, the all ones vector is loaded into both registers as an initial condition [8]. Then, different shifts from the all ones vector are applied to get additional codes. Low cross-correlation codes are important in multiple access because they minimize mutual interference among

the different users in the system. Several sets of preferred pairs of m-sequences that give Gold codes with low cross-correlations may be found in [8].

C. "User 's Bank Codes " Sub-VI

The "User's Bank Codes" sub-VI as shown in Figure 4.7 is composed of twenty different "Gold Code Generator" sub-VI's that output a Gold code for each of the twenty possible users of the system. Each code has a period of 127 bits. It is necessary to produce this many bits for each code, independent of the length of the frequency word (the number of bits used per hop frequency), to ensure that the cross-correlation properties of the codes follow the properties stated in the previous section. The Gold codes are tied to an array building block which creates a 20x127 two- dimensional array output of Gold codes. The dimensions correspond to the number of users and the code length. The Gold codes are then passed to an array selector block where the array index corresponding to the code length is disabled. By doing this, the Gold code corresponding to a given user may be retrieved with its index value which is given by the value of the User ID. For example, if user number four needs to transmit, the User ID number is set to 3 -- note that index values start from 0.

D. "Frequency Synthesizer " Sub-VI

The "Frequency Synthesizer" sub-VI shown in Figure 4.8 takes the number of hopping frequencies and converts them to binary frequency words. A binary frequency word is the binary equivalent of the number of hopping frequencies in decimal. For example, if the number of hopping frequencies is 100, the frequency word will have a length of $\lceil \log_2 100 \rceil = 7$. This sub-VI keeps track of the frequency word changes by converting them to their decimal values. The decimal value conversion is done by the for loop. This value serves as the index value of

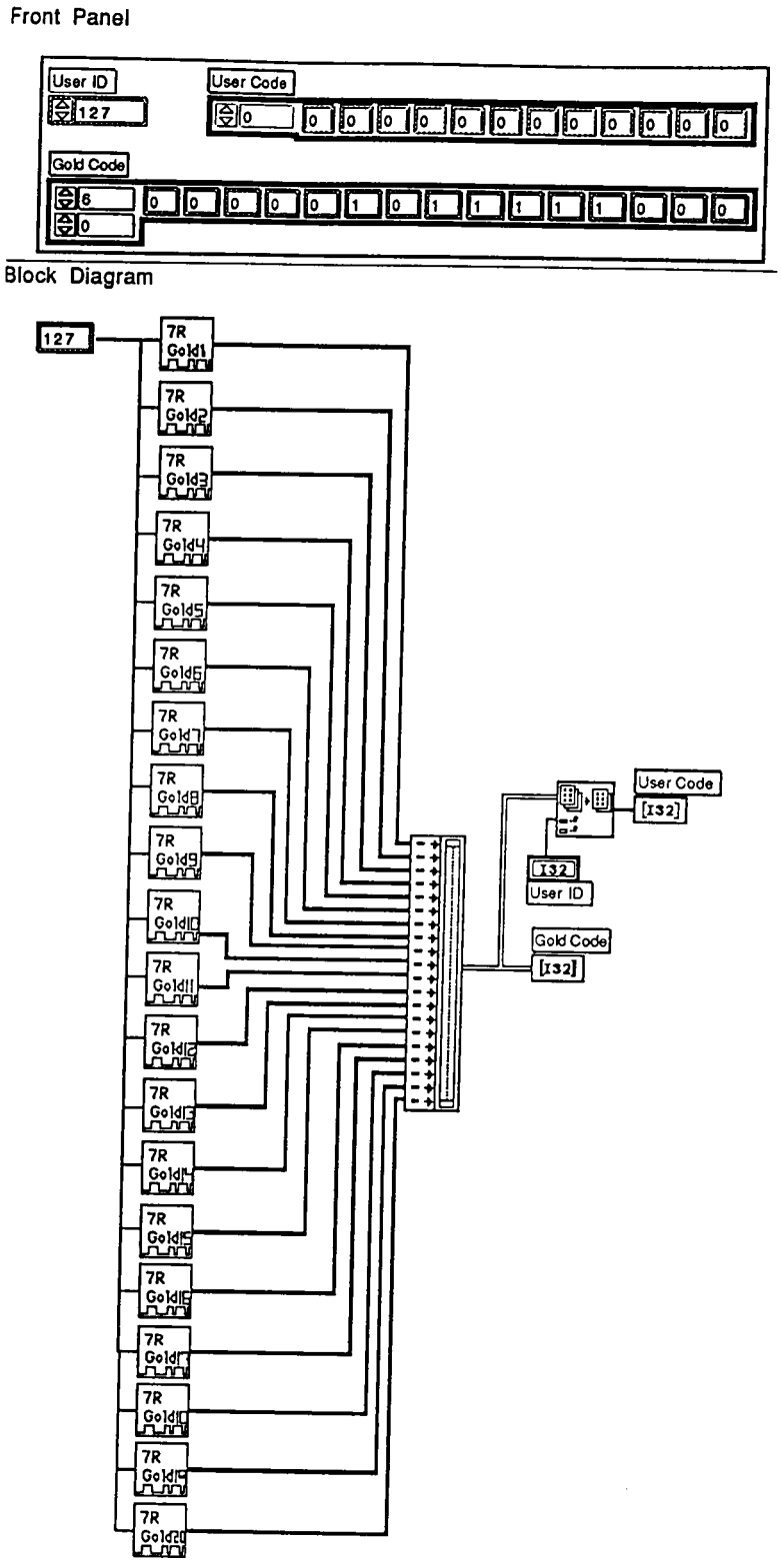
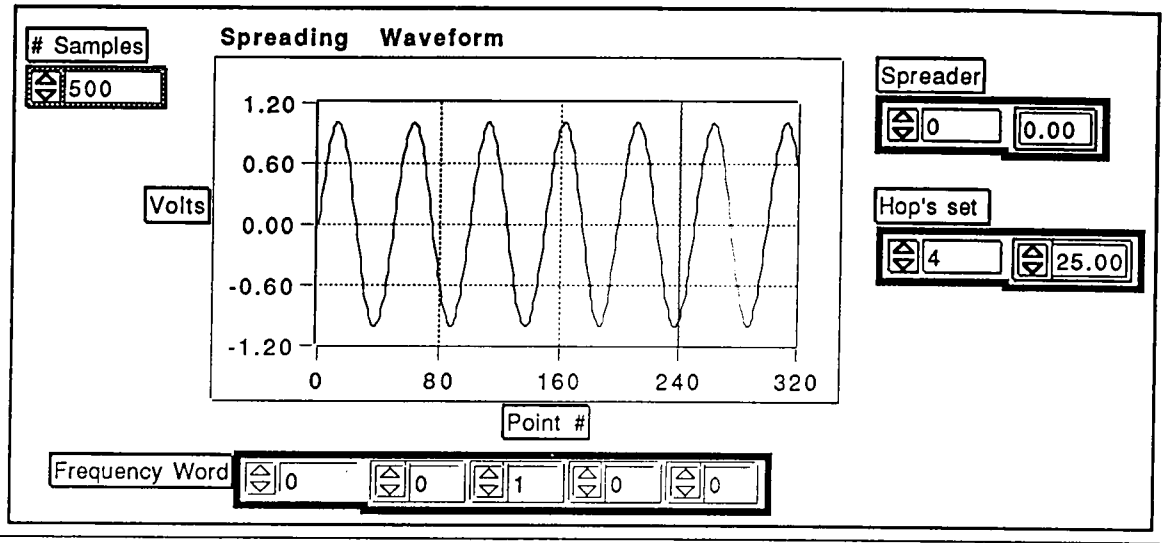


Figure 4.7 "User's Bank Code" sub-VI

Front Panel



Block Diagram

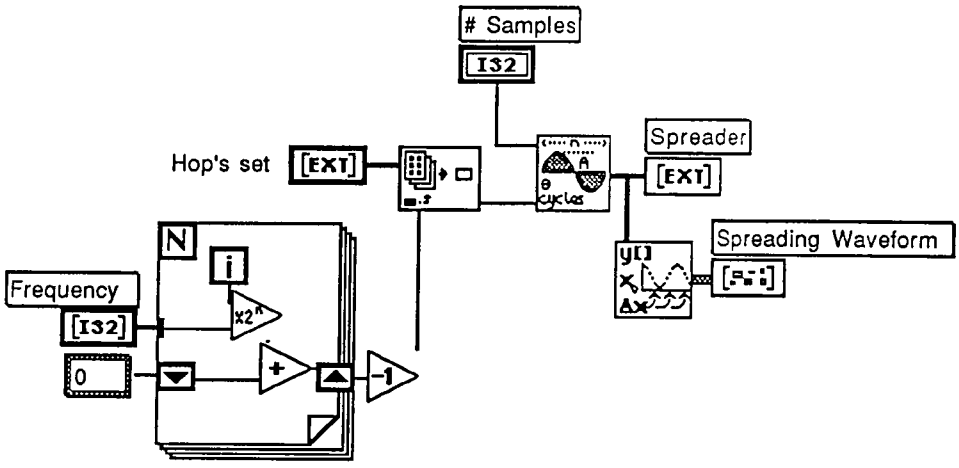


Figure 4.8 "Frequency Synthesizer " Sub-VI

the transmission frequency from the set of all possible hopping frequencies.

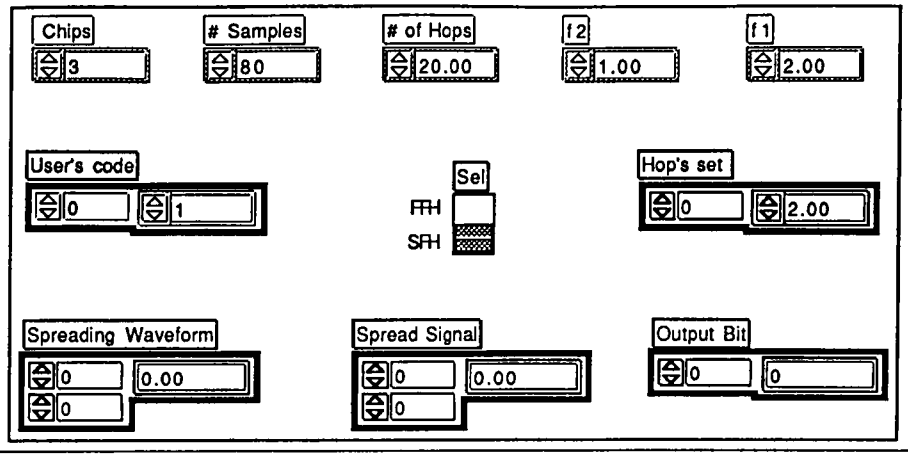
E. " Spreader" Sub-VI

The "Spreader" sub-VI as shown in Figure 4.9 takes the BFSK signal generated from the "BFSK" encoder sub-VI and multiplies it by a sinusoidal signal of frequency f_q from the frequency *hop's set* to generate a spread spectrum signal. The selection of the frequencies depends on the user's code and the mode of transmission. Thus, two case structures are necessary for the two modes of operation.

The true case represents the FFH mode of operation. In this mode, the frequency hopping rate is greater than the information bit rate; therefore, an information bit should be transmitted as many times as determined by the number of chips input value. For example, if the number of chips is 3, the same information bit is transmitted at three different frequencies. The received *user's codes* are passed through an "Array Split" sub-VI (the one with an arrow passing through a stack of window-like blocks) which output the bits of a frequency word to the input of the "Frequency Synthesizer" sub-VI, the one represented by the "Syn." icon. The word frequencies changes for each chip because the starting index for the word frequency within a *user's code* change every time a frequency chip is transmitted, as shown by the loop index attached to the "Array Split" sub-VI. However, the SFH mode of operation, the false case, the word frequency is the same for all the bit chips. Thus, the index of the "Array Split" sub-VI does not need to be changed until the next set of bit chips are sent.

This sub-VI provides two outputs, the spreading waveform, which is a sinusoid of frequency equal to the hop transmission frequency, and the spread signal, which is the result of multiplying the spreading waveform by the message signal. This is basically the spread spectrum signal.

Front Panel



Block Diagram

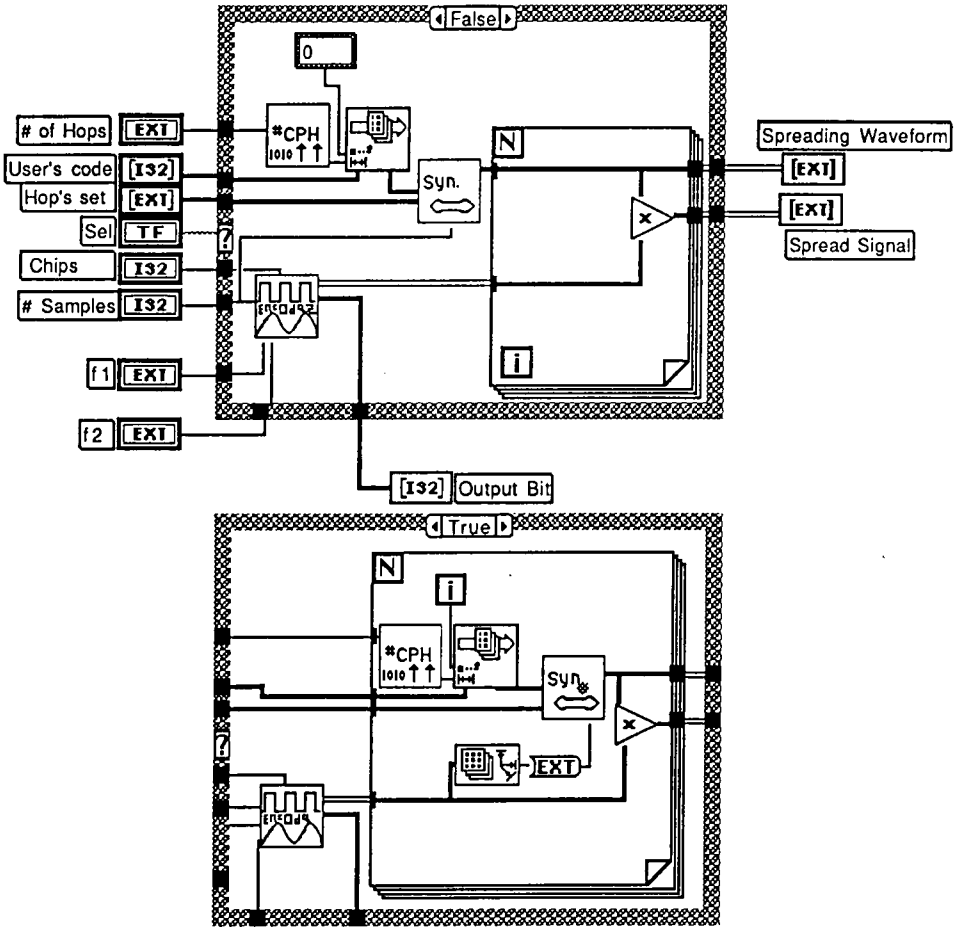


Figure 4.9 "Spreader " Sub-VI

4.3.2 Channel Sub-VI's

The main "Channel" sub-Vi is represented by Figure 4.10. The purpose of this sub-VI is to create discrete multipath delay signals between the transmitter and the receiver with Rayleigh fading amplitudes and then add them to the AWGN present in the channel.

The multipath signal delays are created by feeding first a number of zeros to the transmitted signal array. The number of zeros results from the multiplication of the transmitter signal samples by a random number between zero and one to ensure that the number of samples created this way is less than or equal to that of the transmitted signal. The reason for this constraint is to discard any signal whose delay is larger than a bit duration. To account for the Rayleigh fading degradation of the signal amplitude due to the multipath delays, Rayleigh distributed random amplitudes are multiplied by the transmitted signal amplitudes. In LabVIEW, there is no Rayleigh function generator; therefore, the uniform function generator was used to generate the Rayleigh distributed random amplitude. This may be done by using the percentile transformation method of generating an arbitrary random distribution from the zero-to-one uniform distribution. Mathematically, the transformation takes this form [17]:

$$x_i = F_x^{(-1)}(u_i) \tag{4.5}$$

where x_i is Rayleigh distributed, u_i is uniform distributed, and $F_x^{(-1)}(u_i)$ is the composite function of the Rayleigh cumulative distribution function (CDF) with parameter u_i. Thus, taking the Rayleigh CDF $F_x(x)$ with variance equal to one, the equivalent transformation is obtained:

$$F_x(x) = 1 - e^{-x^2/2} \quad \Rightarrow \quad F_x^{(-1)}(u) = \sqrt{-2ln(1-u)} \tag{4.6}$$

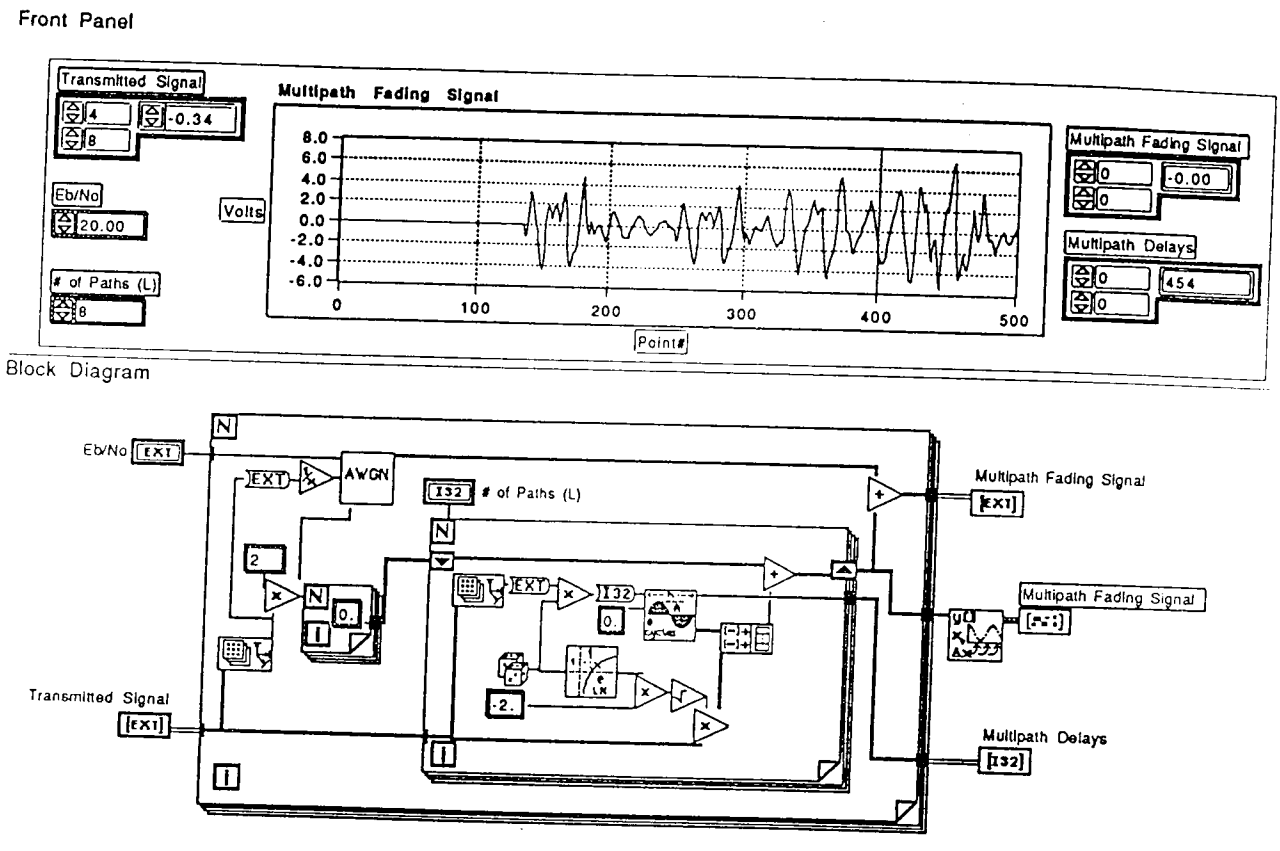


Figure 4.10 "Channel" Sub-VI

Replacing *1-u* by *u* results in the sequence,

$$x_i = \sqrt{-2 ln u_i} \tag{4.7}$$

which has a Rayleigh distribution. This sequence may be generated in LabVIEW because all of the operations in the sequence are in the LabVIEW library.

All of the multipath signals in the signal path are added to each other and to the AWGN to form the received signal at the receiver antenna. The "AWGN" generator sub-VI is shown in Figure 4.11. It takes a signal to noise ratio (E_b / N_0) in dB and produces an AWGN of variance

$$\sigma^2 = \frac{N_0}{2} \tag{4.8}$$

where $N_0 / 2$ is the double-sided power spectral density of the noise.

4.3.3 Receiver Sub-VI's

Some of the receiver sub-VI's are the same as in the transmitter, such as the "Frequency Synthesizer" sub-VI, and the "Despreader" sub-VI; thus, they have already been discussed in section 4.3.1. Figure 4.12 shows the LabVIEW implementation of the receiver. First the *Hp's Set* for the user of interest is determined. This is represented by the *Despread Signal* in the block diagram. The random delays are initialized with respect to the delay of the user of interest. This is accomplished by monitoring the delays of the user of interest and then by putting them in the array "Max" and "Min" functions of LabVIEW and then by taking the minimum value which represents the shortest delay value from the transmitter to the receiver of interest. This delay is set as the zero delay reference upon which all the other delays are based. Upon adjusting the received signal delays, the received signal is multiplied by the *Despread Signal* of the user of interest. Here is where the detection process really begins. Non-coherent

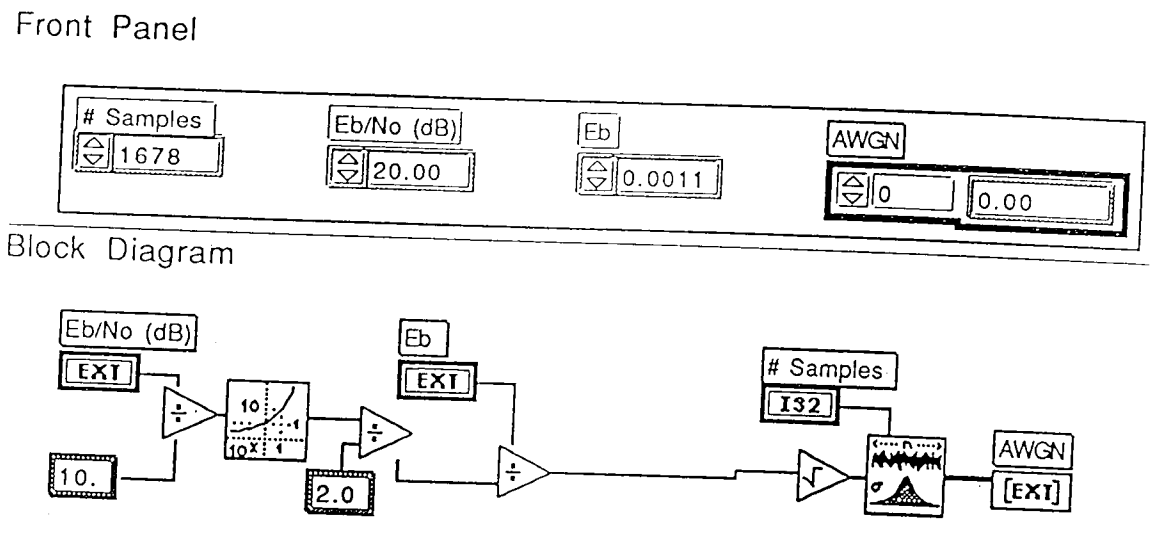
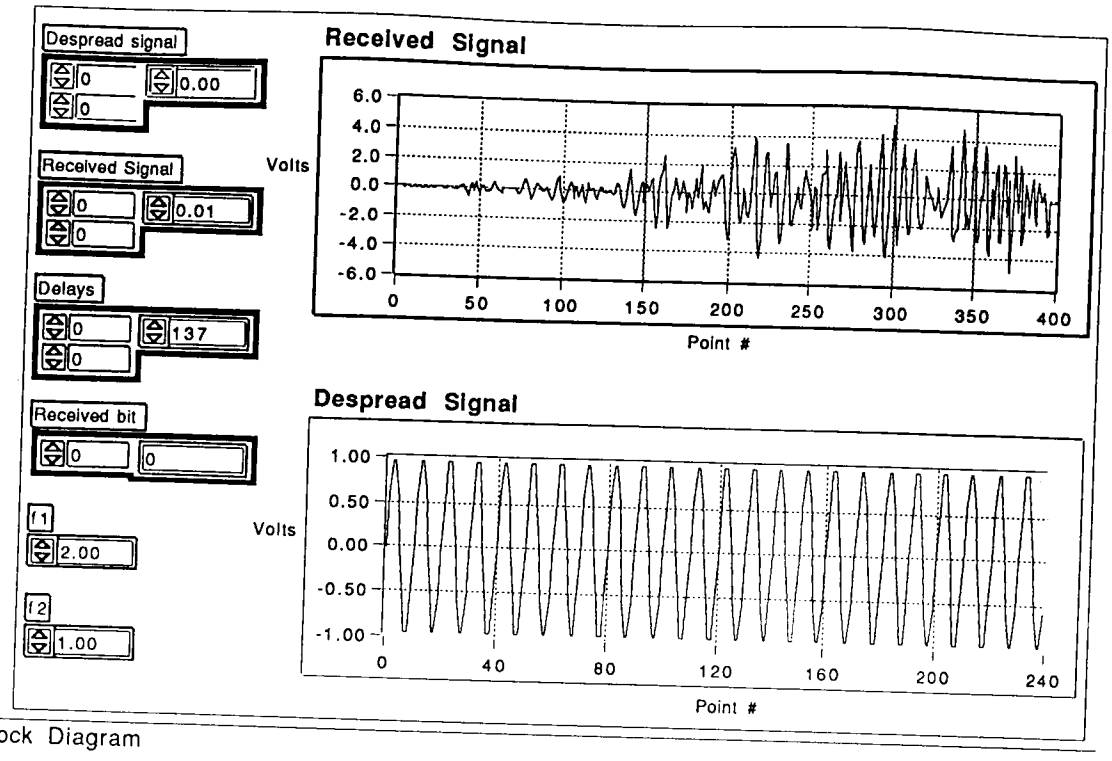


Figure 4.11 "AWGN" Sub-VI

Front Panel



Block Diagram

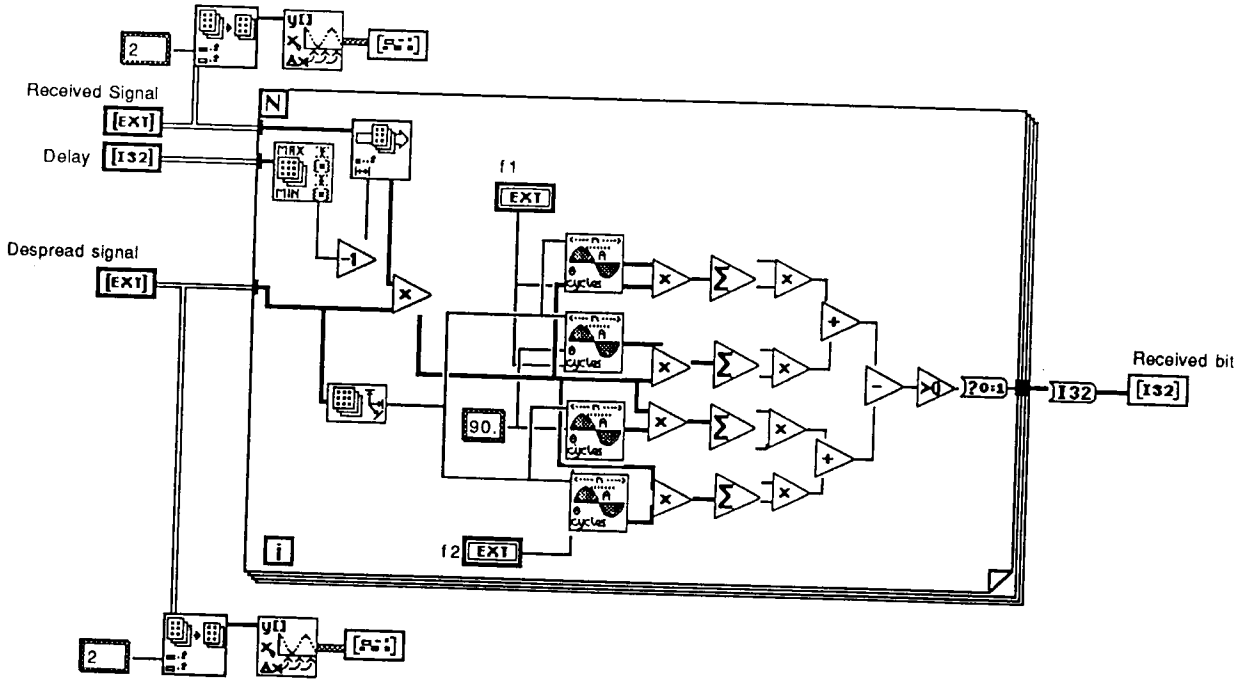


Figure 4.12 "Receiver" Sub-VI

detection is generally used for FSK because it is simpler to implement than coherent detection at the expense of higher BER. Non-coherent detection is achieved by a quadrature detector. Figure 4.13 shows the schematic diagram of a quadrature detector. The detector has two channels, the in-phase (I) and the quadrature (Q). The upper two branches are configured to detect the signal with frequency f1 which corresponds to an encoded binary bit of "1" because the signal at the detector input is multiplied by a sine and a cosine wave of frequency f1. In the same manner, the lower two branches are configured to detect the signal with frequency f2 which corresponds to an encoded binary bit of "0" because the signal at the detector input is multiplied by a sine and a cosine wave of frequency f2. It is important to maintain the tone spacing between the two BFSK signals to $1/T$ to maintain orthogonality so that the product integrator of the branch that matches the received signal is considerably greater than the rest of the branches, thus leading to the correct output value at the decision stage. For example, if a sine wave was transmitted with frequency f2, the lower branch should yield the maximum output, and the other branches should yield near zero values because the reference signal of those branches should be nearly orthogonal to received signal.

For noiseless cases, the receiver operates flawlessly, but as the noise increases, the BER increases as well. The performance of the system will be discussed in more detail in the next chapter.

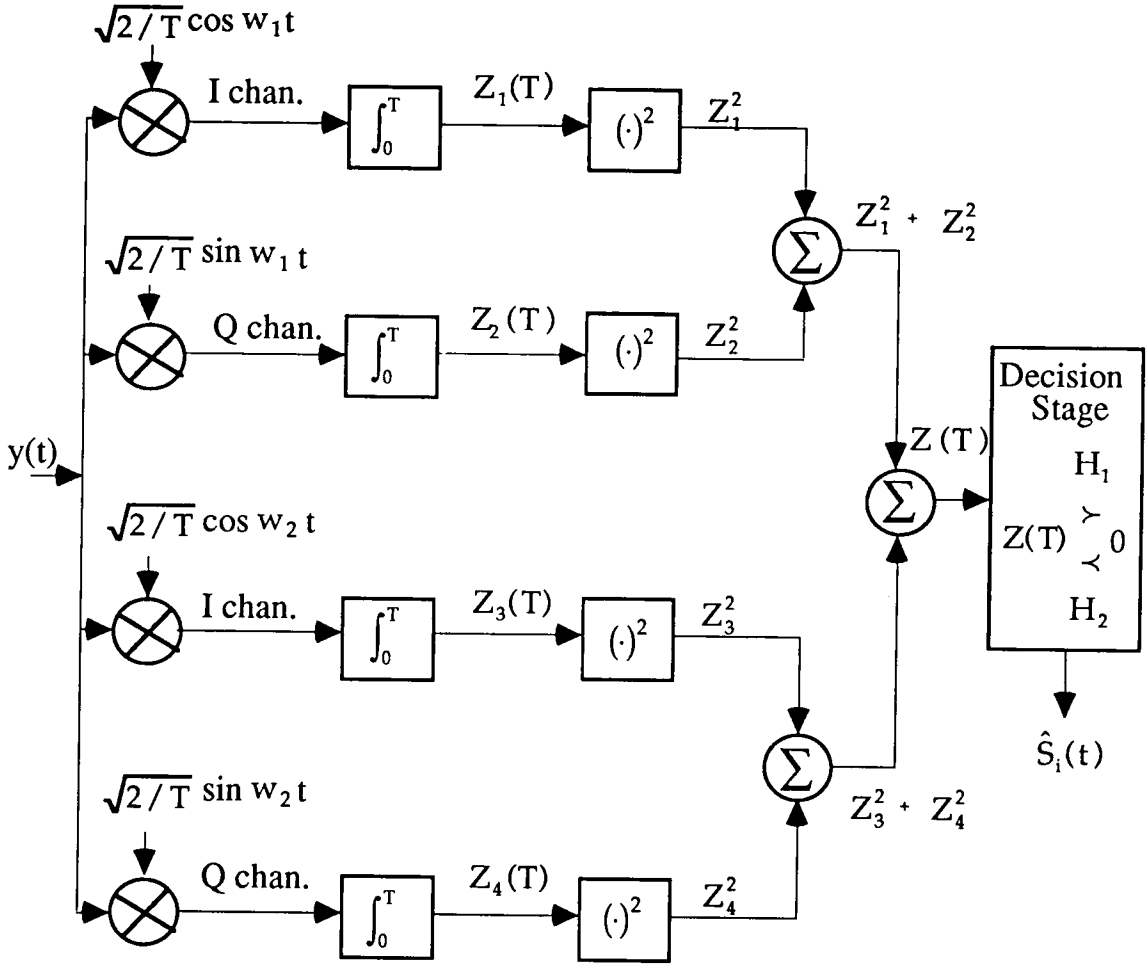


Figure 4.13 Schematic representation of a Quadrature Receiver

Chapter 5

FH/BFSK/CDMA Performance

5.1 Performance Evaluation

In the previous chapter, a computer simulation of the FH/BFSK/CDMA was developed. In this chapter, actual results of the simulation from the variation of various parameters that affect the performance of the system will be obtained and compared to theoretical results. As stated earlier, the performance measurement criteria will be based on the bit error rate (BER) fluctuations as system parameters like number of users, the number of hopping frequencies, and number of chips take on different values. Results are obtained by varying other parameters while letting the parameter of interest remain constant.

Since the system is a multiple access one, a major concern is the mutual interference or multiple access interference (MAI) that results when one or more non-reference users transmit at the same frequency simultaneously as the reference user. This is an event known as a hit. A non-reference user is any user other than the receiver expects. For the system under consideration, after a hit, the demodulator output is equally likely to be any one of the two possible symbols ("1" or "0"). Thus, as more users access the system, it becomes more difficult for the receiver to decode correctly the message of the reference user. Hence, the MAI increases.

Assuming that K multiple access users of the FH/BFSK/CDMA operate over a spread spectrum band with p transmission frequencies, and L number of paths between a multiple access user and the receiver, a mathematical expression that relates all those parameters for the determination of the BER may be obtained. However, an exact mathematical expression for the BER of the system

described above is hopelessly complex and requires prohibitive amounts of computation for its evaluation. Thus, a sub-optimal approximation that lessens the amount of computation for the evaluation of the BER was presented in [13] and will serve as the basis for the performance evaluation in this presentation. The first step for the determination of the BER is to approximate the probability P_i that a non-reference user will transmit in the same frequency band as the reference user by [13]:

$$P_i = \begin{cases} 1/p & lower \quad bound \\ 3/p & upper \quad bound \end{cases} \tag{5.1}$$

The above formula is given in terms of the likelihood of a single hit from a non-reference user. Practically, any combination of the non-reference users may interfere at any given time with a reference user. Thus, considering all the ways a group of *K-1* interfering users may be arranged to interfere with the reference user, the BER due to multiple access interference *P(MAI)*, may be expressed mathematically as [13]:

$$P(MAI) = \begin{bmatrix} K-1 \\ k_i \end{bmatrix} (P_i)^{k_i} (1-P_i)^{K-1-k_i} \tag{5.2}$$

where k_i is the number of interfering users.

The next step is to calculate the signal to interference density ratio. The signal energy is the energy of the signal of the reference user while the interference includes the usual background or thermal noise (AWGN) with single side power spectral density of N_0, the multipath fading of the indoor environment, and the multiple access interference from the *K-1* non-reference

users. The signal to interference density ratio γ may be expressed mathematically as [13]:

$$\gamma = \left\{ \left\{ \frac{E_b}{N_0} \left[1 + (L-1)/2 \right] \right\}^{-1} + \frac{k_i L}{L+1} \right\}^{-1} \tag{5.3}$$

where E_b is the energy of the user of interest which is $\frac{\alpha^2}{2} T$ (note that α is the amplitude of the signal and T is the period). Upon the adjustment for the signal to interference density ratio, it is now possible to calculate the probability of error $P_e(k_i)$ for Rayleigh fading channel [13].

$$P_e(k_i) = \frac{1}{(2+\gamma)} \tag{5.4}$$

Finally, combining the contribution from MAI and channel conditions, the BER for the system may be expressed mathematically in the following way [13]:

$$BER = \sum_{k=0}^{K-1} P_i(MAI) P_e(k_i) \tag{5.5}$$

All theoretical results will be based on the above derivations. It is important to note that the bit rate and the frequency hopping rate for the derivation are the same. Therefore, the comparison of the actual and experimental results presented in the next section will be fair only if the bit rate is the same as the frequency hopping rate. The other cases are presented to show an improvement or performance degradation from the aforementioned case.

5.2 Experimental Results

In what follows, the simulated results of the FH/BFSK/CDMA are presented. The BER is determined from averaging ten runs. This is necessary because different BERs result from each run. A representative result is only possible by averaging all the results over a number of runs. The BER is a function of E_b / N_0 or the ratio of the bit energy of the reference user to the one sided power spectral density of the background or thermal noise energy (AWGN). Thus, all results will be presented in terms of E_b / N_0.

Figure 5.1 shows the case where there is no multiple access interference, the number of chips is equal to one, the frequency hopping rate is equal to the bit rate. The number of paths is ten and the number of hopping frequencies is

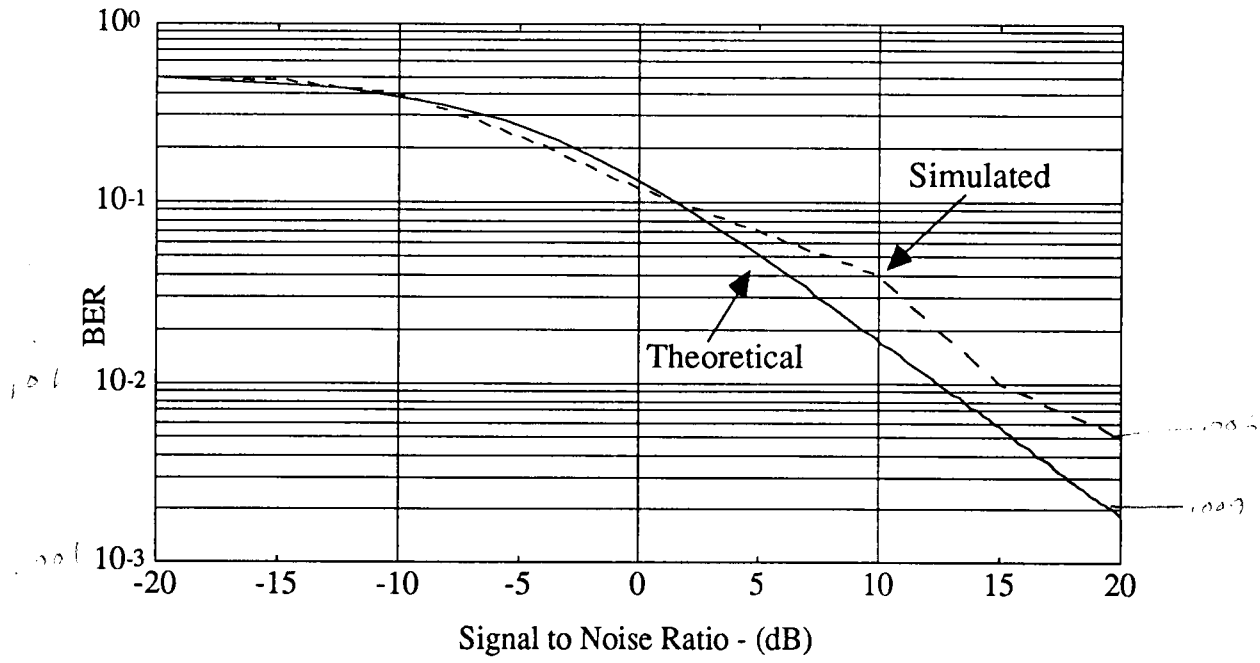


Figure 5.1 Theoretical and Simulated BER for L=10, K=1, p=20, 1 hop/bit.

twenty. This is relative a very low number of hopping frequencies compared to actual systems, which may employ as many as a million frequencies. So, it is not a surprised that at 20 dB of signal to noise ratio, (see Figure 5.1) the BER of the system is still less than 10^{-3}. In Figure 5.2, all the parameters from the previous figure are the same except the number of users has increased from one to six. The effect of the MAI due to the five non-reference users on the system is a severe degradation of the system performance. In fact, at 20 dB of signal to noise ratio a BER degradation by a factor of a hundred from the case of no MAI (Figure 5.1) is observed. The advent of such high BER will render any system worthless under normal conditions. Under such circumstances, an increase in the number of hopping frequencies or in the number hops per bit can improve the performance of the system. The number of hopping frequencies available to the system is crucial in frequency hop systems. As stated earlier, the processing

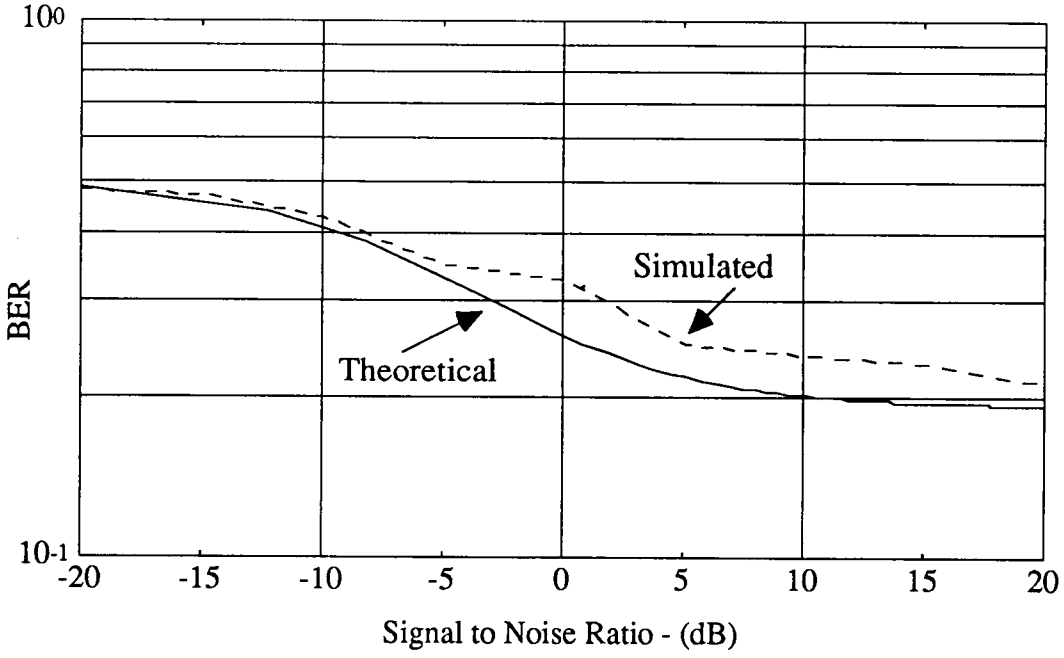


Figure 5.2 Theoretical and Simulated BER for L=10, K=6, p=20, 1 hop/bit.

gain G_p or the ability of spread spectrum systems to withstand channel impairments is roughly equal to the number of hopping frequencies. Observe that in Figure 5.3 after increasing the number of hopping frequencies by a factor of three over the previous figure, a factor of two and seven tenths improvement of the BER at 20 dB was achieved; just three tenths short of the three fold predicted by the processing gain. Another simple way to improve the performance without implementing sophisticated coding algorithms is to increase the number of hops per bit of information. This is done at the expense of decreasing the energy per bit if the data rate is maintained constant, otherwise reduce the bit rate for a constant bit energy. Figure 5.4 shows the case where the hop rate is five times the bit rate. Here the energy per bit was reduced to maintain a constant data rate as in the previous runs. This technique provides a form of diversity by sending the same information bit at different frequencies

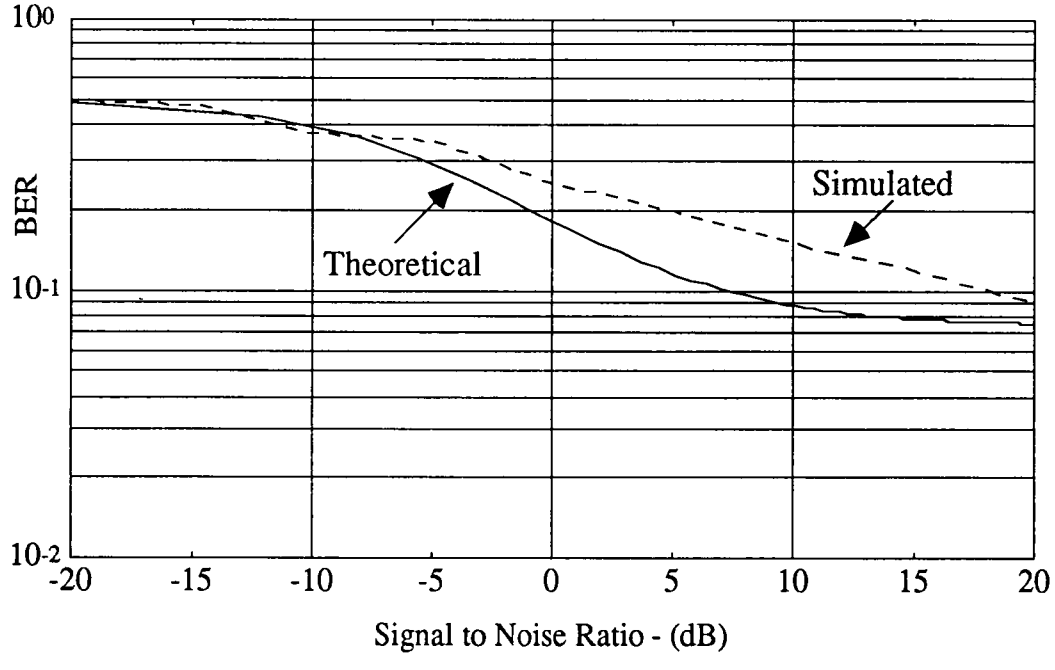


Figure 5.3 Theoretical and Simulated BER for L=10, K=6, p=60, 1 hop/bit.

(five in this case). Hence, the probability of a hit is less likely. Note that the simulated BER shows an improvement over the theoretical of one bit per hop case.

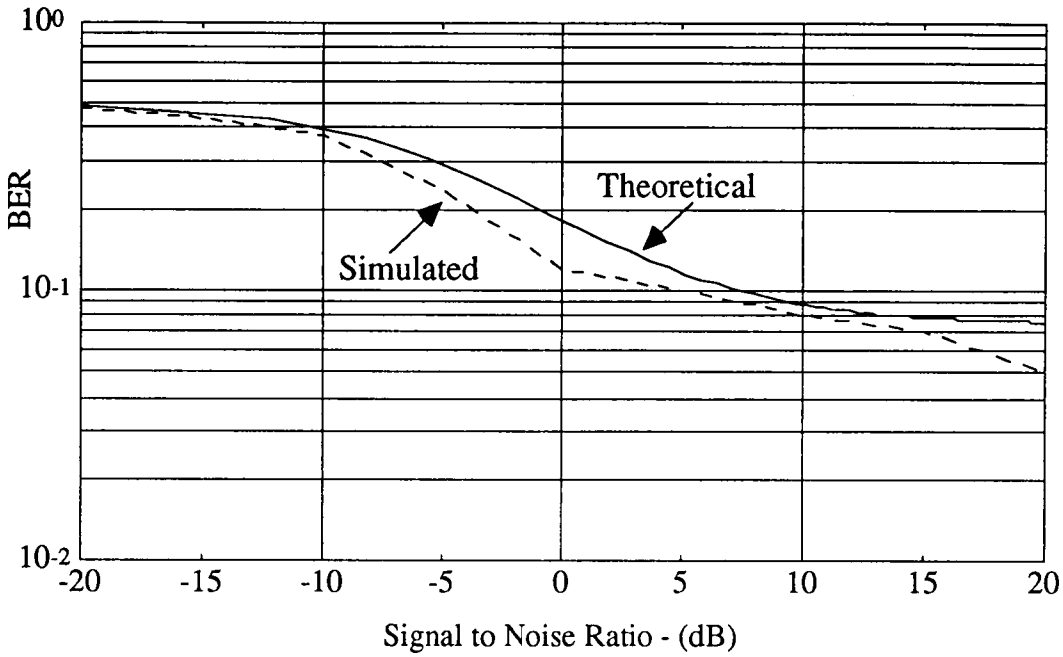


Figure 5.4 Theoretical and Simulated BER for L=10, K=6, p=60, 5 hops/bit.

Figure 5.5 is a departure from the analysis conducted so far where the frequency hopping rate is greater or equal to the data rate -- Fast Frequency Hopping (FFH) mode. This figure is the case where the bit rate is greater than the hopping rate -- Slow Frequency Hopping (SFH) mode. Obviously, there is a performance degradation compared to the one bit per hop. Any interfering user operating in the same band as the reference user can destroy as many as three data bits at a time. Therefore, SFH is usually used in conjunction with DS/SS to form a hybrid system. Such hybrid systems are useful because the DS/SS systems are better for multiple access than FH/SS systems [9]. On the other hand,

bandwidth expansion techniques favor FH/SS systems to achieve higher processing gains than DS/SS systems which translate to better resistance against interference [5]. A hybrid system incorporates both qualities.

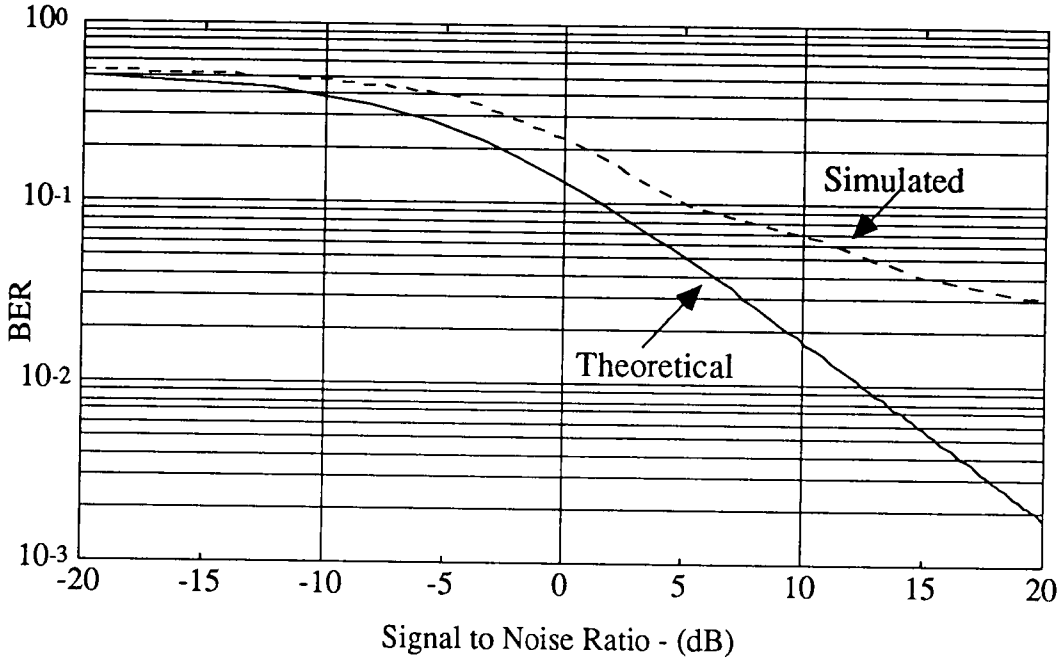


Figure 5.5 Theoretical and Simulated BER for L=10, K=6, p=60, 3 bits/hop.

The simulated results are some what higher than the theoretical results, except for the case in Figure 5.4 which was intended to compare the improvement of the BER of the simulated case of five hops per bit to the theoretical case of one bit per hop. A possible explanation in the disparity of the results rest in the approximation of the bounds used in (5.1). The bounds simplify the mathematical expression, but they are generally accurate within some specified limits. Another explanation lies in the generation of the Gold codes to select the hop frequencies. Although the algorithms to select the transmission frequencies were selected to minimized the hit among the users in the system, depending on the word length, (word lengths are calculated by

taking the greatest integer of the logarithmic in base two of the number of hopping frequencies) some users will have the same grouping of bits sometimes as others. This results in hits and thus higher simulated BER.

For both simulated and theoretical data, the performance of each may be improved by increasing the number of hopping frequencies, or increasing the number of hops per bit. In addition, diversity combining, adaptive equalization and various forms of channel coding may be used to enhance the system performance. Thus, FH networks may effectively be used to counter the effects of multipath fading in the absence of MAI. When there is MAI, to achieve equivalent performance, some type of performance enhancement is necessary.

Chapter 6

Conclusion

The potential cost saving and their ease of installation compared to wired systems are the driving forces behind the increasing interest of indoor wireless networks. However, the success of these networks in penetrating the indoor environment is a function of their performance as well. The indoor environment is hostile to radio propagation because of multipath fading which is a great source of performance degradation. Yet, wireless networks are expected to support the 10 Mb/s speed adequate for today's wired LANs and higher speeds envisioned for the future, offer low delay, good reliability and security against unauthorized users. Thus, in choosing any viable wireless network technology all those factors have to be taken into consideration.

The spread spectrum system simulation developed in this thesis was intended to test the ability of frequency hop spread spectrum to counter the effect of multipath fading under the worst case scenario possible, that is, a Rayleigh fading channel. As the results of the simulation reveal in the absence of multiple access interference the BER performance of the system is very good. On the other hand, when multiple access is present due to additional users sharing the available bandwidth, the BER of the system degrades considerably. The performance of the system may be improved by using more hopping frequencies, or by utilizing various forms of diversity and signal processing (i.e., adaptive equalization) techniques. What is clear, some type of performance enhancement should be used in wireless indoor radio systems when multiple access interference is present. For the system simulated in this presentation, a form of

frequency diversity may be achieved by using more hopping frequencies per information bit. By increasing the number of hopping frequencies per information bit, significant BER improvement is achieved over the case of one hop frequency per information bit.

As stated earlier, the performance evaluation in this presentation was based on the BER performance of the FH/BFSK/CDMA system without regard to its throughput (speed). There are currently spread spectrum systems operating in the vicinity of 5 to 10 Mb/s. Clearly, this is an area that needs further research to upgrade the speed in excess of 10 Mb/s if these systems are to be competitive in the indoor arena.

List of References

List of References

[1] Thomas A. Freeburg, "Enabling Technologies for Wireless In-Building Network Communication", IEEE Communication Magazine, pp. 58-64 April 1991.

[2] Dale Buchholz, Paul Odlyzko, Mark Taylor and Richard White, "Wireless In-Building Network Architecture and Protocols", Proceeding of the IEEE International Conference on Communications, pp. 1025-1031, 1992.

[3] K. Pahlavan, "Wireless Intra-Office Networks", ACM Transactions on Office Information Systems, Vol. 6, No 3, pp. 277-302, July 1988.

[4] George R. Cooper and Raymond W. Nettleton, "A Spread Spectrum Technique for High-Capacity Mobile Communications", IEEE Transaction on Vehicular Technology, pp. 264-275, November 1978.

[5] Bernard Sklar, "Digital Communications Fundamentals and Applications", Prentice Hall, New Jersey, 1988.

[6] Jack T. Taylor and Jim K. Omura, "Spread Spectrum Technology: A solution to the Personal Communication Dilemma", IEEE Communication Magazine, February 1991.

[7] Don J. Torrieri, "Principle of Secure Communication Systems", Artech House, Boston, 1992.

[8] R. C. Dixon, "Spread Spectrum Systems", John Wiley & Sons, New York, 1976.

[9] David L. Nicholson, "Spread Spectrum Signal Design", Computer Science Press, Maryland, 1988.

[10] Matthew Twiggs, "Performance of a Direct-Sequence Code Division Multiple Access Cellular Network", Master of Science Thesis in Electrical Engineering, The University of Tennessee, Knoxville, December 1992.

[11] Rajamani Ganesh and Kaveh Pahlavan, "Statistical Characteristics of Partitioned Indoor Radio Channel", Proceeding of the IEEE International Conference on Communications, pp. 1252-1255, 1992.

[12] "LabVIEW 2 User Manual", National Instrument Corporation Corporation, Austin, Texas, 1990.

[13] Jiangzhou Wang and Marc Moeneclaey, "Performance of FFH Spread Spectrum Multiple Access for Indoor Wireless Communications", Proceeding of the IEEE International Conference on Communications, pp. 1358-1362, 1991.

[14] Theodoro S. Rappaport, Scott Y. Seidel, and Koichiro Takamizawa, "Statistical Channel Impulse Response Models for Factory and Open Plan Building Radio Communication System Design", IEEE Transactions on Communications, Vol. 39, No 5, pp. 794-807, May 1991.

[15] Adel A. M. Saleh and Reinaldo A. Valenzuela, "A Statistical Model for Indoor Multipath Propagation", IEEE Journal on Selected Areas in Communication, Vol. 5, No. 2, pp. 128-137.

[16] Theodore S. Rappaport, "The Wireless Revolution", IEEE Communication Magazine, November 1991.

[17] Athanasios Papoulis, "Probability, Random Variables, and Stochastic Processes", McGraw-Hill, New York, 1991.

[18] Rajamani Ganesh and Kaveh Pahlavan, " On the Modeling of Fading Multipath Indoor Radio Channels", IEEE Globecom, Vol. 3, pp. 1346-1349, 1989.

[19] Rajamani Ganesh and Kaveh Pahlavan, " Statistical of Short Time Variations of the Indoor Radio Propagation", Proceeding of the IEEE International Conference on Communications, pp. 1-9, 1981.

Vita

Aquilino Benjamin Orichi-Batajolo was born in Malabo, Equatorial Guinea on October 6, 1965. He graduated from High School in 1986. In 1986-87 academic year, he worked as a substitute teacher for math and physic in Santa Teresita High School. In Spring of 1988, he entered the University of Tennessee, Knoxville, and graduated with the Bachelor of Science degree in Electrical Engineering in December, 1991. The following Spring semester, he was admitted to the University of Tennessee graduate school to pursue a Master of Science degree in Electrical Engineering, and received his Master of Science Degree in Electrical Engineering in August, 1994.